

**TESTING THE EFFICACY OF GOLD NANOPARTICLES
SYNTHESISED USING *WITHANIA SOMNIFERA* AGAINST
MYCOBACTERIUM SMEGMATIS BIOFILMS**

Thesis submitted in partial fulfillment of the requirement for the
degree of Masters of Science

In

Biotechnology

By

NIDHI TYAGI (217831)

Under the supervision of

Dr. Rahul Shrivastava

To



Department of Biotechnology & Bioinformatics
Jaypee University of Information Technology Wahnaghat,
Solan-173234, Himachal Pradesh

DECLARATION

I hereby declare that the work presented in this report entitled “**Testing the efficacy of gold nanoparticles synthesised using *Withania somnifera* against *Mycobacterium smegmatis* biofilm**” in partial fulfillment of the requirements for the award of the degree of **Master of Science in Biotechnology** submitted in the Department of Biotechnology & Bioinformatics, Jaypee University of Information Technology, Waknaghat is an authentic record of my own work carried out over a period from June 2022 to May 2023 under the supervision of **Dr. Rahul Shrivastava** Associate Professor, Department of Biotechnology and Bioinformatics, Jaypee University of Information Technology, Solan, Himachal Pradesh.

I also authenticate that I have carried out the above mentioned project work under the proficiency stream.

The matter embodied in the report has not been submitted for the award of any other degree or diploma.

NIDHI TYAGI, 217831.

This is to certify that the above statement made by the candidate is true to the best of my knowledge.

Rahul Shrivastava

Associate Professor

Department of Biotechnology and Bioinformatics

Dated:



CERTIFICATE

This is to certify that the work reported in the M.Sc. Biotechnology thesis entitled “**TESTING THE EFFICACY OF GOLD NANOPARTICLES SYNTHESISED USING *WITHANIA SOMNIFERA* AGAINST *MYCOBACTERIUM SMEGMATIS* BIOFILMS**”, submitted by **Ms. Nidhi Tyagi (217831)** at **Jaypee University of Information Technology, Wagnaghat, India**, is a bonafide record of her original work carried out from July 2022 to May 2023 under my supervision. This work has not been submitted elsewhere for any other degree or diploma.

Dr. Rahul Shrivastava

Associate Professor

Department of Biotechnology and Bioinformatics,

Jaypee University of Information Technology,

Place: Solan, Himachal Pradesh.

Date: 15.05.2023

ACKNOWLEDGEMENT

First and foremost, I would like to express my sincere gratitude to the Department of Biotechnology and Bioinformatics, JUIT for giving me consistent support and guidance and support throughout the project process.

I would like to express my deepest gratitude to my supervisor, **Dr. Rahul Shrivastava**, Associate Professor, Department of Biotechnology and Bioinformatics, Jaypee University of Information Technology, Solan, Himachal Pradesh. I am been extremely fortunate to have a guide, who consistently provided me with the liberty to explore my potential and for providing me such a good lab environment.

I would also like to thank Dr Deepak Sharma sir and PhD scholars of the department, especially Ayushi Sharma ma'am who have been a pillar of support from the very start and have kept me motivated to complete my project.

Last but not the least, I would like to thank my friends and classmates for constant support, helping hand and care when times were hectic.

Thank you

Nidhi Tyagi

(217831)

TABLE OF CONTENT

Declaration	ii
Certificate	iii
Acknowledgement	iv
Table of content	v – vi
List of Abbreviations	vii – viii
List of Figures	ix – x
List of Tables	xi
Abstract	xii
Introduction	1-4
Aims and Objectives	5
Review of Literature	6 – 31
Materials and Methods	32 – 41
Bacterial strains	33
Media and other Chemicals	33
Instruments used	33
Streaking	34
Gram staining	35
Ziehl-Neelsen Staining	35
Preparation of plant extract	36
Preparation of nanoparticles	36
Ratio optimization	36
pH optimization	37
Temperature optimization	37
Time optimization	37
Antimicrobial Susceptibility Testing(AST)	37
MIC of green synthesised gold nanoparticles	38 – 39
Biofilm Assay	40 – 41
Crystal Violet assay	40
CFU count assay	41

Results	42 – 53
Simple streaking	43
Quadrant streaking	43
Gram staining	44
Ziehl-Neelsen Staining	44
Preparation of plant extract	44
Preparation of nanoparticles	45
Ratio optimization	45
pH optimization	46 – 47
Temperature optimization	47
Time optimization	48
XRD results	48
FTIR results	49
DLS results	50
Zeta Potential results	51
Antimicrobial Susceptibility Testing(AST)	52
MIC of green synthesised gold nanoparticles against <i>E. coli</i>	53
MIC of green synthesised gold nanoparticles against <i>M. smegmatis</i>	54
Crystal Violet Assay of <i>E. coli</i> biofilms	55
Crystal Violet Assay of <i>M. smegmatis</i> biofilms	56
CFU count assay	58
Discussion	58 – 60
Conclusion and future prospects	61
References	62 – 70
Appendix	71– 73
Publications	74 – 75

LIST OF ABBREVIATIONS AND ACRONYMS

%	Percent
ATP	Adenosine Triphosphate
Au	Gold
AuNPs	Gold Nanoparticles
Cm	Centimetre
CV	Crystal Violet
DH	Decahedral
DLS	Dynamic Light Scattering
DNA	Deoxyribonucleic acid
Fcc	Face centred cubic
FTIR	Fourier Transform Infrared Spectroscopy
GPL	Glycophospholipids
HAuCl₄	Gold(III) Chloride
HR-TEM	High Resolution Transmission Electron Microscope
Ic	Icosahedral
IR	Infrared Spectroscopy
IT	Information Technology
LAM	Lipoarabinomannan
M	Metre
MDR	Multiple Drug Resistant
Mg	Microgram
Min	Minute
ml	Millilitre
mm	Millimetre
NaCl	Sodium Chloride
NaOH	Sodium Hydroxide
NIR	Near Infrared region
Nm	Nanometre
NPs	Nanoparticles

°C	Degree Celsius
OD₆₀₀	Optical Density at 600nm
Pa	Pascal
Psi	Pound-force per square inch
PXRD	Powdered X-Ray Diffraction
Rc	Critical nuclei
Rh	Hydrodynamic particle size
ROS	Reactive Oxygen Species
Rpm	Round Per Minute
Sec	Second
SEM	Scanning Electron Microscope
SPR	Surface Plasmon Resonance
TEM	Transmission Electron Microscope
UV-Vis	Ultraviolet- Visible
XRD	X-Ray Diffraction

LIST OF FIGURES

Fig 1: Different stages of Biofilm Formation	9
Fig 2: Cycle of Biofilm	9
Fig 3: Green synthesis of nanoparticles using plant extracts	23
Fig 4: Mechanism of nanoparticles to inhibit biofilm	26
Fig 5: Microtiter plate depiction for MIC and antibiofilm assay	39
Fig 6: Simple streaking of <i>E.coli</i>	43
Fig 7 (a): Quadrant streaking of <i>M. smegmatis</i>	43
Fig 7 (b): Quadrant streaking of <i>E. coli</i>	43
Fig 8 (a): Gram staining of <i>E. coli</i>	44
Fig 8 (b): Ziehl-Neelsen staining of <i>M. smegmatis</i>	44
Fig 9: Preparation of <i>Withania somnifera</i> water extract	44
Fig 10: Colour of reaction mixture before and after 4 hours of incubation at 30°C.	45
Fig 11: Colour change after 4 hours of different ratio.	45
Fig 12: UV-Vis spectra of different samples for ratio optimization of ratio of plant extract and salt solution	46
Fig 13: Colour change after 4 hours of different pH	46
Fig 14: UV-Vis spectra of samples with different pH of plant extract	47
Fig 15: UV-Vis spectra of nanoparticles incubated at different temperature	47
Fig 16: UV-Vis spectra of nanoparticles at different time period.	48
Fig 17: Intensity v/s 2θ graph of XRD	49
Fig 18 (a): FTIR analysis of powdered green synthesised gold nanoparticles.	50
Fig 18 (b): FTIR analysis of suspended green synthesised gold nanoparticles.	50
Fig 19 (a): Particle diameter [nm] v/s distribution [%] graph of DLS	51
Fig 19 (b): Zeta potential v/s relative frequency graph of Zeta potential analysis	51
Fig 20: Zone of inhibition shown by green synthesised nanoparticles of <i>E. coli</i>	52
Fig 21: Zone of inhibition shown by green synthesised nanoparticles of <i>M. smegmatis</i>	52

Fig 22: Fig 22: Microtiter well plate for testing MIC of <i>E. coli</i>	53
Fig 23: Microtiter well plate for testing MIC of <i>M. smegmatis</i>	54
Fig 24: Crystal Violet assay to study biofilm inhibition of <i>E. coli</i>	55
Fig 25: Crystal Violet assay to study biofilm inhibition of <i>M. smegmatis</i>	56
Fig 26: CFU Count assay of <i>M. smegmatis</i> biofilms	57

LIST OF TABLES

Title	Page Number
Table 1: Important terminologies related to nanotechnology	16 – 17
Table 2: List of microbes used in this study	33
Table 3: List of Chemicals	33
Table 4: List of Instruments	33
Table 4: Different ratio of plant extract of <i>W. somnifera</i> and 1M H ₂ AuCl ₄	36
Table 5: OD ₅₇₀ readings of <i>E. coli</i> to determine MIC	53
Table 6: OD ₅₇₀ readings of <i>M. smegmatis</i> to determine MIC	54
Table 7: OD ₅₇₀ of <i>E. coli</i> to determine biofilm inhibition	55
Table 8: OD ₅₇₀ of <i>M. smegmatis</i> to determine biofilm inhibition	56
Table 9: CFU/ml in 10 fold dilutions of control and test wells for testing biofilm inhibition of <i>M. smegmatis</i>	57

ABSTRACT

Drug resistant bacteria pose a pronounced effect on public health globally. Biofilm are associated with numerous persistent infections making them resistant towards antibiotics. Formation of Biofilm by pathogenic bacteria provides supplementary challenge for their treatment. Green synthesis of nanoparticles using plant extracts involves use of bio molecules found in them to reduce the metallic ions in nano material. Plant based green synthesis has provided marvellous advantages over physical or chemical methods of synthesis of nanoparticles. Plant based green synthesis have demonstrated other well known biological properties such as antimicrobial, anti-inflammatory, antioxidant, anticancer, anti aging and wound healing effects. Gold nanoparticles has acquired more emphasize because of their biocompatible nature, optical properties and surface functionalization. In this study, we have focused on antibiofilm activity of plant mediated synthesis of gold nanoparticles against *Mycobacterium smegmatis*.

Key words; Biofilm, Gold nanoparticles, Plant based green synthesis, *Withania somnifera* *Mycobacterium smegmatis*.

CHAPTER 1
INTRODUCTION

1.1 Introduction

In biofilm microbes are able to pose strong tolerance and resistance towards antibiotics [1]. Extent of resistance depends on which mode they have acquired for biofilm. Biofilm can contribute to antibiotic resistance by providing physical barrier which prevents the entry of antibiotics across them [2]. Antibiotics can bind to various positively and negatively charged molecules present in EPS like glycoprotein, proteins, glycolipids, eDNA and uronic acid[3,4]. Other factors limiting the absorption of antibiotics by constituents of biofilm and their degradation by some hydrolase enzyme like β - Lactamase [5, 6]. Pel polysaccharides are cross linked to eDNA which is negatively charged and thus provide structural basis and protection to invading microbes [7, 8]. Antimicrobial resistance has emerged as a significant public health issue especially because of the reduced discovery of new secured antimicrobial drugs [9, 10]. Numerous strategies have been employed to strengthen the currently offered antimicrobial chemotherapeutic alternatives [11, 12].

Nanotechnology deals with development and application of materials at nanoscale range (1-100 nm). Materials show unique characteristics at nanoscale level which are not exhibited by bulk counterparts. Difference in properties arises because of the high ratio of surface area to volume of nanoparticles which gives them a heightened reactivity that affects their mechanical and electrical properties. This shows that behaviour of materials at this range is governed by quantum effects leading to variation in optical and electromagnetic properties [13].

Overall, every naturally occurring and man -made systems has basal level of organisation at nanoscale. It may constitute nanocrystals, nanotubes and nanomotors. Nanotechnology gives an account how atoms are assembled or disassembled in an object along a scale of length. Bio based nanomaterials are of great applications now a day because of their ability to show some intrinsic properties, functionality and response more precisely as compared to bulk material. This gives a groundbreaking opportunity to improve the productivity of already known substances [14].

Nanomedicine is a term used to describe combination of science and technology to prevent, diagnose and treat disease by utilization of nanomaterial that are synthesised particularly to perform required functions. Nanomedicine has grown new strategies for the treatment and diagnosis of various diseases. Miniaturization of drug particles is of great importance because they increase surface area of drug so that it can dissolve easily. Porosity is other important factor for entrapping gases. Nanoparticles can be employed to carry drug molecules; their

drug carrying ability depends on size and bioavailability. Nonmaterials can deliver drugs intravenously and can pass through even small blood vessels in body [15].

Nanomaterials can be combined with drugs and biomolecules which give an advantage of slow and controlled drug release. Their size helps to enhance their penetrating ability among tissues which helps to overcome physiological barriers and avoid degradation of drugs inside body. Nanotechnology has application in monitoring, prevention, diagnosis and cure of various diseases by different mechanisms. Nanotechnology-based approaches are expected to provide a promising breakthrough in tackling drug-resistant pathogenic bacteria that form biofilms. Studies have reported for the usage of nanoparticles coated with biofilm inhibiting agents. Size of nanoparticles is good enough to cross biofilm layer. Nanoparticles can damage microbial cell wall. Their longer plasma half life and drug loading capacity provides additional advantage to target biofilm forming cells. To deliver required biomolecules nanosystems like microemulsions, solid lipid nanoparticles, nanoemulsions, liposomes, metallic nanoparticles cyclodextrins, and polymeric nanoparticles are utilised. Such nano-structured systems are thought to be useful against the infectious microbes that become resistant to typical treatment methods [13, 16].

Naturally occurring substances in plants and microbes have ability to reduce the metal salt and by changing the components of reaction mixture and physical parameters, they could lead to production of nanoparticles with different shape and size. Biological synthesis has proved to be advantageous in biomedical applications like for drug delivery. Biologically synthesised nanoparticles are eco-friendly and much more cost effective [17].

Gold is supposed to be more biocompatible to be used in diagnostics and therapeutics now a day in bioscience. Biologically synthesised gold nanoparticles were proven as good catalyst and do not require artificial surfactant and capping agents at definite and low concentration. Thus AuNPs offer function as non toxic system for delivery of drugs and genes. In GNPs, monolayer offer tuning of surface characteristics like hydrophobicity and charge, while gold core contribute to stability. AuNPs show interaction with thiol groups present in biomolecules thus released selectively and effectively intracellularly [17].

AuNPs have been widely investigated for their antimicrobial properties, specifically against mycobacterium like *Mycobacterium tuberculosis*. Nevertheless, the effectiveness of AuNPs in combating mycobacterial biofilms is currently being actively researched, and there is only limited information available on their efficacy in this domain. *Mycobacterium smegmatis* can be used as model organism for mycobacterial species. In this study we have synthesised gold nanoparticles using *Withania somnifera* and tested their efficacy against *M. smegmatis*

biofilms. Several studies have shown antimycobacterial activity of *W. somnifera*. So, water extract of *W. somnifera* was used to reduce the H₂AuCl₄ solution to produce nanoparticles.

1.2 Problem statement

Dealing with rising cases of *M. tuberculosis* is a serious public concern. Inability of antibiotics to cure acute infections has led to increase in treatment time and cost and even mortality rate in several cases. *M. tuberculosis* is a slow growing organism and thus discovering new drugs against it a lengthy process. *M. tuberculosis* is a Biosafety level 3 organisms which offer limitation for research associated with it. So alternatively *M. smegmatis* can be used as it is Biosafety level 1 organism non infectious to humans and can be grown easily in labs. *M. tuberculosis* also forms biofilms which offers protection against many drugs, so special delivery system is required to combat the situation. Nanomaterials can carry our molecule of interest inside the biofilms and kill the invading microbes. AuNPs are being used because of their penetrative ability of microbial cell structures, augmentation of cell membrane damage, disrupt bacterial DNA and release ROS.

Due to increasing prevalence of infections caused by pathogenic microbes and resistance offered by them to antibiotics, there is an immediate need to create new antimicrobial agents to combat clinical pathogenic infection. The colonization and infection process involves important steps such as biofilm formation and invasion into host cells. Therefore, we conducted a study to evaluate the effectiveness of using gold nanoparticles (AuNPs) to inhibit pathogenic growth and prevent biofilm formation on *M. smegmatis*.

1.3 Aims and Objectives

1. To synthesise gold Nanoparticles using *W. somnifera*, their optimization and characterization.
2. To check antimicrobial susceptibility of *Escherichia. coli* and *Mycobacterium smegmatis* against green synthesised Gold nanoparticles.
3. To check biofilm inhibition activity of green synthesised Gold nanoparticles against *E. coli* and *M. smegmatis*.

CHAPTER 2
LITERATURE SURVEY

2.1 Biofilm

A biofilm is a consortium of microbial populations aggregated to form a 3-D mesh-like structure growing on a biotic or abiotic surface [18]. Biofilm may consist of single or different microbial communities which are arranged in a complex layout and assist favourable conditions to the inhabiting microorganisms when they are under some stressful environment. The architecture of biofilm may consist of living and dead bacterial cells, extracellular polymeric substances (EPS), and other biomolecules excreted by the cells [19]. Extra Polymeric Substance can contribute up to 90% of the total organic carbon content in a biofilm and is regarded as the principal polymer composite in a biofilm which is primarily composed of polysaccharides [20]. The constituents of the Extracellular Matrix (ECM) are dependent upon the inhabiting microbes and the external environmental conditions. Biofilms are wrapped by the extracellular matrix which provides them a way to adhere to a surface; aggregation of microbes utilizes nutrients and provides a way for the confinement of water within microbial cells. The extracellular matrix can provide an obstacle to drugs and thus empower the microbes to pose excessive resistance to antibiotics and other chemicals used to kill bacteria. Microbes associated with biofilms show different characteristics from their respective planktonic state. Microbes tend to transcribe different genes when they are in freely suspended form. Sessile bacteria in biofilm show different mechanisms for their attachment initially to a suitable surface, communicating with other bacteria and developing a proper structure and environment, and thereafter their detachment [21].

Table1. Composition of Biofilms

Components	Percentage in EPS
Cells of microbes	Approx 2-5%
Carbohydrates	Less than 1-2%
Proteins and Enzymes	Less than 1-2%
DNA/ RNA	Less than 1-2%
Water	97%

2.2 Biofilms related infections

Bacterial biofilm found to be responsible for nearly 80 percent of persistent and enduring pathogenic organisms inside the human body. Micro - organisms in biofilm seem to be more than thousand times untreatable than free swimming cells. The biofilm which develops on biomedical implants, such as catheters, heart valves, dental units, joint prostheses, contact lenses, and intrauterine devices, can cause bloodstream and urinary tract infections. Such Kind of infections can only be recovered by expelling the implanted material and implanting new one, which is quite challenging to the patients and also adds on the expenses of treatment [22].

A wide range of biofilm-forming bacteria are responsible for causing disease including *Pseudomonas aeruginosa*, *Mycoplasma pneumoniae*, *Staphylococcus epidermis*, *M. tuberculosis*, *Mycobacterium abscessus*, *M. smegmatis* etc., It has become major health concern because of their recalcitrant behaviour towards antibiotics and easily evade from host immune system. Some bacteria like *P. aeruginosa*, *Staphylococcus aureus*, *Acinetobacter baumannii*, and many other microbes forming a biofilm over the surface of injected medical devices which makes them 1000 times additional tolerant and resistant to drugs. Medical devices are a major pathway for entry of most pathogenic bacteria, they can be found on contact lenses, ortho-dental prosthetics, pacemakers, and urinary catheters [23].

2.3 Stages formation of a biofilm

Bacteria within a biofilm may attach to a biotic or abiotic surface reversibly by adhesion or irreversibly by cohesion. Formation of a biofilm is a complex and robust process; microorganisms within biofilm have evolved different biochemical methods based on the availability of nutrients and stress. There are four major stages involved in formation of biofilm; (1) attachment, (2) growth, (3) colonization and (4) dispersal. A distinctive group of genes are transcribed to support the formation of biofilm which enhances the production of polysaccharides, fatty acids, proteins, and glycopeptidolipids [24].

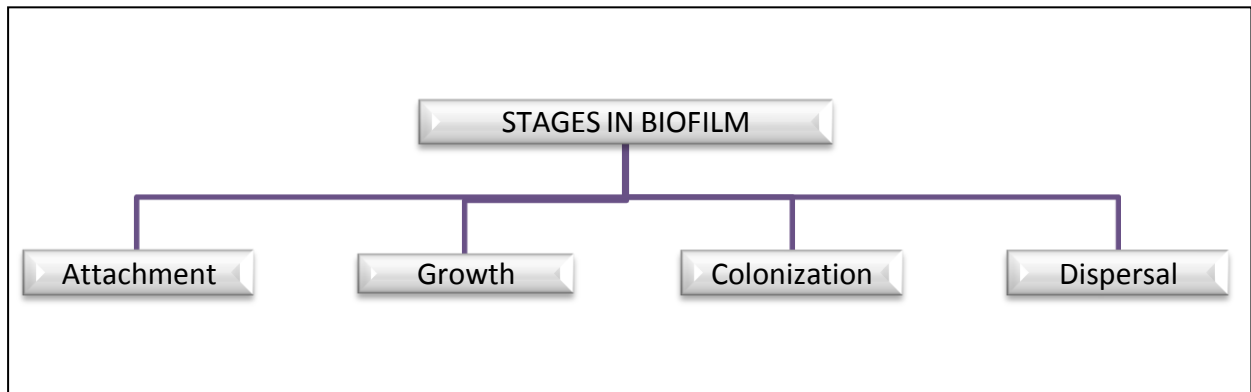


Fig 1: Different stages of Biofilm Formation

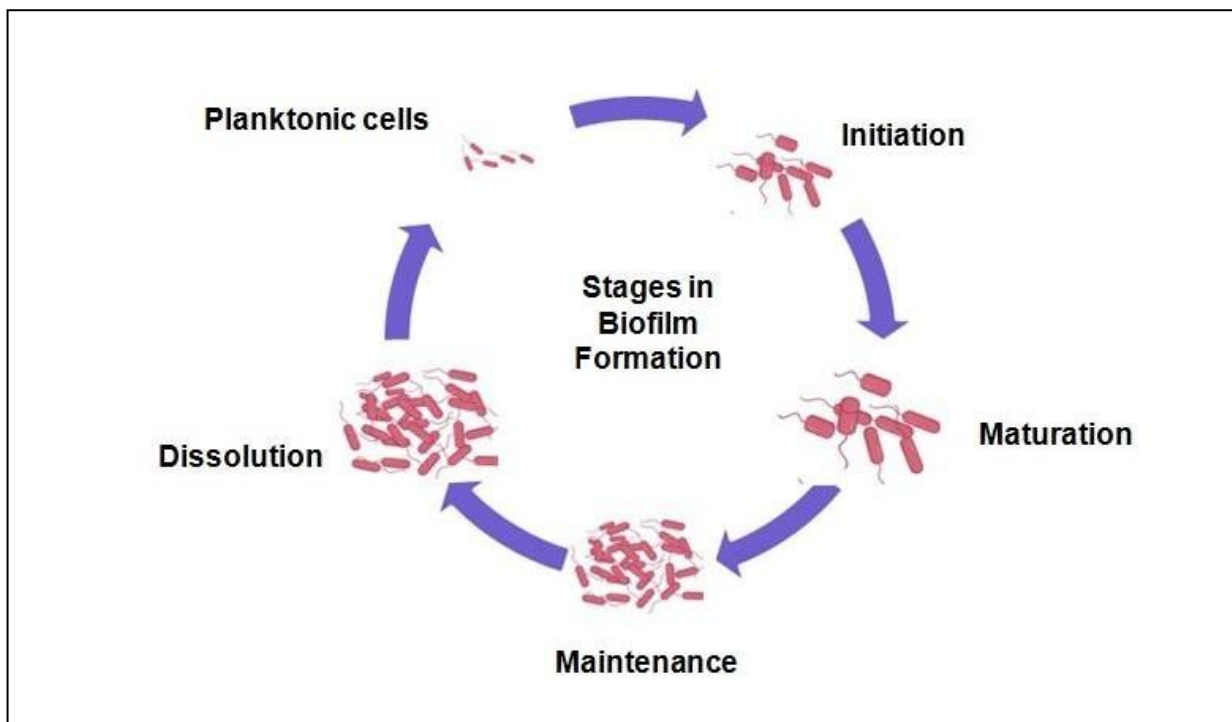


Fig 2: Cycle of Biofilm

2.3.1 Attachment: Initially bacteria are bound loosely that can detach easily and turn back to planktonic phase. These attachments are brought about by electrostatic interactions between the surface and bacteria, which is aided by the participation of adhesions on pili of bacteria. Early adhesion is hugely affected by hydrostatic pressure induced by medium viscosity and the lack or involvement of any chemotactic molecule [24].

After attachment to the substratum, microbes go for micro colony formation and develops external matrix using EPS leading to development of biofilm. Consecutive development may be reversible or irreversible. Flagellated bacteria have an additional advantage of having flagella which experience hydrodynamic stress and promote biofilm formation. In case of living host, attachment is governed by interaction between bacterial proteins and carbohydrates and proteins present extracellularly on host tissue or cell. It is majorly affected by the hydrophobicity of these two membranes. Some adhesion molecules like Sag are found to stick with collagen of eukaryotes and thus provide a place for the cells to cling and aggregate [25].

After attachment, some auto-inducer signals regulate the expression of genes leading to up regulation of factors which encourage sessile colony formation. Genetic alteration in *Bacillus subtilis* and *Listeria monocytogenes* has shown fine regulation of genes such as SinR and PrfA respectively [26].

Analysis from phase contrast microscopy has shown that mutants of *P. aeruginosa* that are unable to attach on surface, have defective type-IV pili and flagella were found to play significant role in formation of biofilm. Many studies also strongly support the fact that surface structures have an important role early attachment of microbes for biofilm development. Attachment is also altered if liposachharides are manipulated. Examining *P. aeruginosa* biofilm formation have shown that this organism first petrol along the surface to find appropriate place for contact initially. Once appropriate location is found they come to rest but time-lapse microscopy revealed that once this microbe forms a single layer above the surface they remain mobile but start twitching movement instead of swimming [26].

2.3.2 Growth Once the attachment of cells to surface is completed thereafter, they tends to undergo accumulate and adapt to a life in a biofilm. Two major changes occur with sessile bacteria i.e. increased the amount of EPS synthesis and enhanced antibiotic resistance. This further provides protection to residing microorganisms and making this as a serious medical issue. Additional characteristics that biofilm bacteria may acquire include improved tolerance to UV radiation, greater rates for exchanging genetic material, increased production of secondary metabolites and modified biotransformation [26].

2.3.3 Colonization Proteins, Exopolysaccharides, extracellular DNA (eDNA), and other substances are secreted by bacteria as a result of colonisation , this improve substrate exchange and nutrient distribution in addition to contributing to structural integrity. Virulence

factors are transmitted through horizontal gene transfer, and their genes are present in plasmid-encoding biofilm. The size and architecture of the biofilm are significantly influenced by the availability of nutrients. Cells which are present at periphery receive more oxygen and nutrients than inner cells which makes a gradient among them leading to bio diversification and variation in metabolism. Cells present outside can grow more rapidly if compared to that of present in inner core. In such conditions the cells which are undernourished attains static development and thus their population is reduced. These latent cells develop resistance for antibiotics and are hard to identify in persistent infections caused by biofilm [27, 28]. Cells of *Candida albicans* inside the external surface evoke genes involved in the translation of proteins necessary for synthesis of cholesterol, glycolysis and formation of external cell wall, meanwhile cells in the central core mostly express genes which are involved in metabolism of sulphur or cell wall disruption. This demonstrates that a biofilm is a dynamic community of cells that can alter their metabolic processes in response to environmental changes, indicating their active nature.

2.3.4 Dispersal: The final stage of the biofilm results in cell dissociation, which spreads clusters of cells or single cells. The dissipation of bacterial biofilm is a set of interconnected event that causes the release of specific cells near the end of the biofilm life span. These lased cells give the bacterium the nutrients it needs to grow and eventually disperse. Genes encoding exopolysaccharides or fimbriae are shut down by cells undergoing dispersal, while genes encoding flagella or chemotactic polypeptides which are obligated for a planktonic lifestyle, are unregulated [29, 30].

2.4 Modulation of Biofilm

Biofilm are formed usually when microbes are in stress conditions; development of biofilm in such unfavourable conditions is an outcome of alteration in expression of genes. It is a struggle of microbes to withstand the external extreme environment. In such circumstances composition, formation and function of biofilm is regulated by a cascade of regulatory mechanisms [31].

2.4.1 Signalling by Nucleotide Secondary Messenger

Nucleotides like cyclic adenosine 3', 5'- monophosphate (cAMP) and 3',5'-monophosphate (c-di-GMP) are vital elements for signal transduction networks, which relate how prokaryotes

perceive their environment to their particular cellular activities. These molecular operations are more important for microbes which bears external unfavourable environment [32]. It has been demonstrated that the new and widely distributed bacterial second messenger c-di-GMP maintains biofilm development in response to environmental stimuli [33, 34]. According to studies, EPS components such pili, polysaccharides, eDNA and flagella help to build biofilm and are controlled by c-di-GMP via certain receptors [35-37].

Additionally cAMP is also present in many prokaryotes and considered to be conserved in different bacterial species. cAMP plays major role in dispersal of *P. aeruginosa* biofilm as well as in production of biofilm by *Vibrio cholerae*. *Salmonella* can establish biofilm at liquid air interface, called pellicle if the medium having low osmolarity at room temperature and fixed incubation is given, while biofilm is formed at solid-liquid junction if minimal media is provided. Such biofilm are called bottom biofilm [38, 39].

As biofilm formation is found to be regulated by nucleotide secondary messengers, cAMP and c-di-GMP using different mechanisms so a study based on signal regulation can aid to disclose the process of biofilm formation. This will further provide new ways to combat infections related to biofilm and their prevention [40].

2.4.2 Quorum sensing

Conversion of a single cell to an association of cells arises a need for intercellular communication of cells within the group to exaggerate their functioning efficacy. This is done by a process named Quorum sensing, it is a collaborative aspect of microbes that helps in the regulation of gene expression and is thought to be crucial for microbes to sustain in extreme conditions [41]. When there is a change in cell density within a population it starts a cascade in which some signalling peptides or molecules like phenol-soluble modules, 3, 5-cyclic diguanylic acid (c-di-GMP), competence stimulating peptides farnesol and rhamnolipids are produced. Quorum sensing assists the microbes to manage the proper density required to produce a pathogenic effect in some organisms like *V. cholerae* [42]. In gram- positive and gram- negative bacteria Quorum sensing is regulated by acyl-homoserines lactones and small peptides respectively. *P. aeruginosa* involves rhamnolipids for maintaining open channels and regulating intercellular interactions in between cellular clusters to facilitate nutrition distribution [43].

2.5 Mycobacterium smegmatis

M. smegmatis was initially isolated by Lustgarten in 1884 and later named by Neumann and Lehmann in 1889. *M. smegmatis* is a bacterium that typically lives in the layers of cells and can form a biofilm when several cells group together. In biofilms these bacteria live in group of cells that adhere to surfaces and are placed in a matrix synthesised by them. *M. smegmatis* is one of the most frequently used non-pathogenic species in the genus *Mycobacterium* and is commonly used laboratory organism used as model for studying mycobacterial physiology, pathogenesis, and genetics. *M. smegmatis* is generally found in water, plants, and soil, and it is known to have a worldwide distribution. This organism is found in sixteen States, Russia, Australia, Switzerland and Canada. This organism is generally considered a group of saprophytes that seldom cause illness and cannot survive in mammalian hosts. If provided with sufficient nutrients, this microbe will have a white, velvety appearance with fine wrinkles. After approximately 48 hours of growth, *M. smegmatis* will proliferate rapidly, resulting in a pigment less velvety yellow colour, different from its original whitish appearance. The external structure of this microbe may appear gloosy, shiny, smooth, coarsely collapsed or wrinkled finely, depending on the conditions. *M. smegmatis* is one of the species of genus *Mycobacterium* that is not found to cause serious illness and grows more rapidly than other species of this genus. This bacterium requires oxygen for respiration, and its energy is mainly produced through oxidative phosphorylation. Although most *Mycobacteria* are obligate aerobes, certain virulent species can undergo anaerobic respiration during infection, where oxygen is not necessary. DNA-binding protein 1 of *Mycobacteria* plays a vital role in the prolonged survival of *M. smegmatis* by coordinating various cellular functions. To eliminate this microbe, it is necessary to identify an appropriate treatment, such as inhibiting the biosynthesis pathway of mycolic acid, which is a crucial step in bacterial cell division. Since the discovery of streptomycin, use of medicinal drugs has been recognized as an effective approach for tuberculosis treatment. However, the therapy for latent and tuberculosis infection typically takes 9 to 6 months, respectively, which can lead to the emergence of drug-resistant strains. The challenges in discovering a drug to treat the infection stem from various obstacles, such as the pathogen's slow growth rate, highly contagious nature, impermeable characteristics, increased virulence and hydrophobicity of their cell envelope. Since infection caused by tuberculosis can be fatal, it is crucial to identify a potential drug to manage the disease. *Mycobacterium smegmatis* shares several characteristics with other dangerous and pathogenic *Mycobacterium* species, including *Mycobacterium tuberculosis*. The key similarity between different *Mycobacterium* species is

the biosynthesis of mycothiol, which is crucial for the production of basic thiol required for their growth [44].

Bacteria can attach to a surface in different ways, such as through reversible and primary adhesion, reversible and secondary adhesion, and biofilm formation. Studies have shown that nontuberculous mycobacteria, including *M. smegmatis*, are commonly present in household plumbing and drinking water distribution systems. These bacteria can attach to pipe surfaces to produce biofilm, forming a high concentration of cells [45].

Bacteria may move or remain stationary on the substrate throughout the adhesion process, and the adhesion itself may be irreversible or reversible. The initial reversible step comprises of weak interactions, such as electrostatic, van der Waals, and hydrophobic forces between the substratum surface and bacterial cell membrane. The subsequent irreversible stage involves the contribution of cellular surface features such as fimbriae and flagella, as well as stronger bonding forces such as covalent and hydrogen bonds. The capability of bacteria to attach to a substrate may be influenced by several factors, including its hydrophobicity, topology and the surface's charge, and the availability of appropriate nutrients. Although some research suggests that the energy of the surface without a substrate can affect bacterial adhesion, such as by enhancing surface roughness and hydrophobicity, it is commonly accepted that microbes tend to attach more quickly to non-polar hydrophobic surfaces compared to hydrophilic substances [45].

2.6 Mycobacterial biofilms

Mycobacterial biofilms can also be explained in similar manner as other biofilms. However, mycobacterial species tend to form biofilm not just on surface, but also at the boundary between the air and culture media. This can be due to presence of different components in extracellular matrix and mycolic acid content of mycobacterial cell wall. Various molecules from cell wall of bacteria such as adhesins mediate primary attachment of bacterial cells to the substrate. After attachment to the substrate bacteria start synthesising extracellular matrix. Mycobacterial cell surface lack pili or fimbriae, rather some proteins are present which help in aggregation of cells to surface and intercellular attachment [46].

Mycobacterial cell wall contains enough hydrophobic lipids like lipopolysachharides, mycolic acid, phthiocerol dimycocerosates, lipoarabinomannan (LAM), glycopeptidolipids, (GPLs) and phenolic glycolipids, which are responsible for biofilm formation, colony morphology virulence and antibiotic resistance of mycobacterium [47].

2.7 Nanotechnology

Nanotechnology has introduced innovations in various fields of science and technology. It deals with atoms and molecules having at least one of their parameter in the range of 1 -100 nm [48]. Nanotechnology and nanostructures are broad and multi-disciplinary domains for study and development that have grown exponentially over the past few years. Recently, a global assessment of current discoveries has revealed a considerable interest in the area of nanotechnology [49]. The international production of nanomaterials has been expanding in recent years, and economists expect this trend to continue. Nanoparticles (NPs) are the most prevalent forms of nanomaterial which may have applications in a variety of products, ranging from automotive industries and nanocomposites in the aerospace industry to everyday items such as food packaging and additives, IT products, sporting goods, cosmetics, electronics, and textiles. Based on current research progress, NPs for biomedical and agricultural applications may become common in the global market in the near future. Especially over the past few years, developing countries have shown interest in production of nanoparticles due to the economic benefits they provide [50].

Humans have broadly used phyto-based sources since former generations for medication for different diseases. Approximately one quarter of currently accessible primary pharmaceutical compounds and their byproducts are derived from natural resources. Herbal compounds with various molecular structures provide a framework for exploring new medications. There is a recent tendency in developing medicines based on natural resources, which involves creating a synthetic lead compound mimicking the chemical structure of the original compound and that is easy to modify. Natural ingredients have fascinating attributes such as incredible heterogeneity of chemical entities, biological as well as chemical features with precision of higher molecular weight molecules, and lesser side effects. This tends to make them favourable leads for the discovery of new drugs. Moreover, the use of bio statistical techniques has aided in forecasting the interactions between drug molecules and the advancement of novel drug molecules and the advancement of novel drug discoveries such as target-driven drug exploration and drug transportation [51].

The traditional usage of intravenous and oral drug molecules to cure disease caused by microbes is fraught with complications. Current medications, involves the usage of elevated amounts of drugs to assure that enough amount should reach the specific target microorganisms, but these approaches are not necessarily advantageous and may result in undesirable adverse reactions which may give rise to resistance to a new drug within the microorganisms. There is a limitation of alternative strategies and treatments to address this

issue; as a result, it is a major source of concern for health professionals and government agencies, with obvious implications for global public health. One approach of dealing with this challenge is the utilization of nanostructures to boost and galvanize the microbicidal efficiency of already available and emerging new drug treatments [52].

Bulk material typically has constant physical characteristics under normal circumstances. However, due to changes in particle shape and size while synthesis; the nanoparticles go through a variety of alterations in electrical, chemical, optical, and magnetic properties. According to the published literature, silver and gold nanomaterials are widely used in the formulation of new drugs, pharmaceutical products, and cosmeceutical and medicinal products [48].

The classical chemical methods of nanoparticles synthesis have several negative consequences, including the release of harmful residues into the natural environment, which negatively impacts the physical conditions of both humans and animals, as well as require proper disposal, otherwise may cause other environmental issues. Furthermore, for effective commercial synthesis, chemical synthesis methods necessitate the use of sophisticated, high-end instrumentation as well as high energy costs [48].

Table 1: Important terminologies related to nanotechnology [53]

Nanotechnology	Nanotechnology pertains to the scientific and engineering disciplines that deal with the synthesis, design, characterization, and implementation of materials and devices whose minimum functional arrangement has at least one dimension in the nanometre scale, which is equivalent to one billionth of a meter. This field involves the manipulation of materials and devices at the nanoscale level, including their synthesis, design, and characterization.
Nanoscale	A scale ranging from 1–100 nm.
Nanomaterial	Nanomaterials possess dimensions that fall within the nanoscale range.
Aspect ratio	The proportion between the length of the main axis and the width of the minor axis can be described as the aspect ratio of a tiny object.
Nanosphere	Nanoparticles having an aspect ratio of 1 can be termed nanospheres.
Nanorod	Nanorod is a term used for a system having longest and shortest axes of different lengths. These are nanoformulations with a range 1 to 100 nm of

	width .
Nanofiber	A nano-sized entity that has two dimensions within the nanoscale and a third dimension that is substantially greater
Nanowire	Nanowires can be considered similar to nanorods, but they have a greater aspect ratio.
Nanotube	The term "nanotubes" refers to nanofibers that have a hollow center.
Nanocomposite	Nanocomposites refer to materials that consist of several components with distinct phases, where at least one of the phases has a size on the scale of nanometers.

2.8 Nanotechnology applications

Nanotechnology offers us the ability to alter the characteristics of the external layer of a capsule, which in turn allows us to regulate the delivery of intended compounds. This capability of controlling the release is particularly valuable in the field of medicine, as it allows for a slower absorption of drugs, targeted delivery to specific body locations, or activation through an external trigger. Nano- and micro- formulations that have the potential to be used in various areas such as food industry to develop nutritionally-enhanced food, vaccines, pesticides, veterinary medicine are currently being created and patented by large food companies, agribusiness like Kraft, Monsanto, and Syngenta. Nano and microcapsules can be designed in various ways, and one such design is slow release, where the capsule gradually releases its contents over an extended period, such as for controlled delivery of substance within the body. Capsule shell can also be designed to release its contents in different ways depending on the intended purpose. For example, it can break upon contact with a surface, when the environment reaches a certain temperature, or in a specific pH environment. Additionally, the capsule can be ruptured by external ultrasound frequency or a magnetic field. A DNA nanocapsule can be used to deliver foreign DNA into living cells to transcribe a specific protein, which is useful for DNA vaccines.

- Specific release - the design of the shell is such that it ruptures upon binding of a specific chemical to a molecular receptor (for instance, when it comes across a protein or tumour in the body).

- Quick-release - upon coming into contact with a surface (such as a leaf being sprayed with pesticide), the capsule shell fractures.
- Heat-release - the shell will only release its ingredients once the temperature in the environment rises above a specific level.
- Moisture release - when water is present, such as in soil, the shell disintegrates and liberates its contents.
- Ultrasound release - the external ultrasound frequency causes the capsule to rupture.
- Magnetic release - when a magnetic field is applied, the capsule's shell is ruptured by a magnetic particle inside it.
- pH release - these nanocapsule is designed to disintegrate solely in an acid or alkaline environment that is specific, such as within a cell or in the stomach.
- DNA nanocapsule - by smuggling a short strand of foreign DNA into a living cell, the capsule can release it and take control of the cell machinery to produce a particular protein, as is the case with DNA vaccines [54].

2.9 Approaches for synthesis of metallic nanoparticles

2.9.1 Top-Down or Destructive approach

Chemical and mechanical fabrication techniques are used in top-down strategy for nanomaterial synthesis. Top-down approaches involve the production of nanomaterials by disintegrating the large particles into smaller ones, generally through milling, etching and attrition. Top-down methods are better suited for producing nanostructured films and nanomaterials having size greater than 100 nm. Such strategies are utilized to create electrical circuits with high connectivity and integration. One such example of top-down approach is the fabrication of an Integrated circuit, in which miniature pieces of machinery (e.g., springs, fluid channels and levers) are integrated into a small circuit. The main disadvantage associated with recently used destructive approach methods is limitation of their minimum resolvable feature size [55].

This method involves separating bulk raw material into particles with nano dimensions using various physicochemical techniques. Physical methods involve managed methods of shaping, milling, and cutting the substances into the aspirated shape and order, using pyrolysis, nanolithography, thermolysis, and radiation-induced methods. However, the disadvantage is that resulting nanoparticles have imperfect surface structures. A disadvantage of using this method is that it can be quite costly due to the significant amount of power needed to maintain the high temperature and pressure conditions [56]

2.9.2 Bottom-Up or Constructive approach

Also known as the constructive approach; it involves the synthesis of NPs generated through the self-assembly of the chemical or biological species may be atoms, molecules, or clusters. This is a less expensive option that gives users more command over the assimilation of the finished product, which has a greater uniform chemical composition, size, and shape.

Constructive synthesis procedures such as chemical electrochemical, sonochemical, and green synthesis are commonly used. Except for green synthesis methods, the limitation offered by this method is the isolation of the nanoparticles which are produced from their reaction mixture, which may contain harmful substances such as organic solvents, toxic chemicals, and other reagents [56].

In contrast to top-down strategy, Bottom-up strategy, allow for the creation of nanomaterials with lesser flaws. This approach involves the integration of atoms, molecules, and other nanoparticles that serve as precursors in such approaches to generate complex nanostructures. Ionic and molecular self-assembly plays an important role in the bottom-up approach wherein van-der Waals forces, noncovalent bonds, such as ionic and hydrogen bonds, and hydrogen bonding mediated by water, are employed to assemble individual blocks/molecules into bigger structures. These approaches enable us to control the composition and properties of the individual component. The size of the building blocks is decided according to the desirable characteristics. Bottom-up strategy includes co-precipitation and wet chemical procedure such as microemulsion and sol-gel methods [55].

2.10 Methods for Nanoparticles Synthesis

1.10.1 Physical Synthesis of Nanoparticles

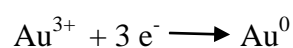
Under the protocol of physical synthesis, there is a semiconductor or metal material being targeted that is situated in a vacuum with a pressure range of 10^{-4} to 10^{-8} Pascal. To create a vapour which is saturated with the elements at the target location, direct heat is applied through methods such as an electron beam or other means. By introducing an inert gas like argon into the vacuum chamber, collisions between metal (or semiconductor) particles and the inert gas occur, leading to the release of atoms. These collisions promote the speedy growth of particles.

The nuclei will have a chance of being dissolved or there are chances that many other atoms are attached to them. This is referred to as the nucleation stage. Eventually, there will be a point where the size of the cluster becomes large enough that adding more atoms to it will

start to become energetically favourable. At this point in the process, when a sufficient number of atoms have come together to form a stable nucleus that can begin to grow into a larger structure, the size of the nucleus is referred to as the critical nuclei, often abbreviated as r_c . Once this critical nuclei stage is reached, the process enters into the growth stage, during which new atoms that enter the surrounding gas will begin to attach themselves to the existing nuclei, causing the nuclei to increase in size and ultimately leading to the formation of a larger crystal or other structure. Evaporation could be used for producing the gold nanoparticles. This growth of nanoparticles is often very rapid. Placing particles on a substrate causes them to rapidly cool, resulting in structures that are typically metastable and not in equilibrium. The lack of time for the particles to adjust to their surroundings before solidification prevents the structure from being completely stable and can lead to changes over time. Due to the distinctive properties of gold and the particular production process employed, it is highly probable that the AuNPs generated through vacuum evaporation will exhibit either icosahedral or decahedral morphology. Gold possesses an exceptional capacity to form intricate and symmetric configurations, and the vacuum evaporation technique offers precise regulation over the dimensions and outlines of the particles. Since Dh and Ic are both fivefold crystal symmetries that can frequently exist at the nanoscale rather than in bulk crystals, this is an extraordinary characteristic of gold nanoparticles. The structure is linked to many fundamental aspects of gold. Many more formations are observed in addition to Ic and Dh spheres. Generally, physical approaches offer the following benefits: - Precise control over particle size. Crystal structure of the nanoparticles can also be controlled. - Improved fabrication conditions. Two drawbacks are associated with this approach. Firstly, it is not easy to transport particles into a suspension as they need to be loaded onto a substrate. Secondly, providing a protective layer to the particles, also known as passivating, is a challenging task [57].

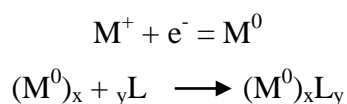
2.10.2 Chemical Synthesis of Nanoparticles

Chemical synthesis relies on the chemical reduction of a metal acid or salt using a reductant compound for example hydrazine, hydrides, ethylene glycol, and citrate. In gold chloride, for example, if we have gold chloride as metal salt the ions of gold are reduced in such a manner that we have :



Following the generation of metal atoms in the reaction mixture, growth and nucleation of particles will be continued, leading in the generation of nanoparticles. The growth ratio is

substantially slower than in the context of evaporation, which is a significant difference. This gives rise to nanoparticles with a structure equivalent to the structure of bulk, which corresponds to the FCC structure in regards with gold. The agent used for reducing is critical for determining the size and crystal structure of the nanoparticles. Nevertheless, numerous additional variables affects the synthesis of NPs, such as the pH, the temperature of the solution, relative concentrations and type of reactants, as well as additional factors that have involved in nanoparticles synthesis are sometimes difficult to control in general. To escape from these factors, the surface of nanoparticles can be stabilized by organic molecules like alkyl amines, alkanethiols, polymers, and citrate ions. These molecules reduce their ability to assemble via electrostatic or steric stabilization. Following equation depicts the reaction involved:



Where (x) represents the number of atoms in the particle, (L) symbolizes the ligand which is used as a stabilizing agent, and (y) is the number of ligand molecules surrounding the nanoparticles [57].

2.10.3 Green Synthesis of Nanoparticles

Numerous techniques are accessible for producing nanoparticles. However, physical and chemical synthesis methods can be costly and produce harmful byproducts. Conversely, the biological approach is affordable, straightforward to produce, diminishes the environmental burden of chemicals, and eliminates irrelevant processing while synthesis. Moreover, it is commonly recognized that physical and chemical techniques are fraught with uncertainties regarding the morphology, dimensions, and distribution of nanomaterials, and above all, they require the use of expensive and hazardous chemicals that contribute to environmental pollution. On the other hand, nanoparticles produced from natural substances are referred to as biogenic nanoparticles, and the procedure for their synthesis is called biological or green synthesis, as it is eco-friendly and sustainable. The process of creating nanoparticles using biomolecules or living organisms that function as both reducing and capping agents is known as biological synthesis. This can involve either prokaryotic or eukaryotic cells [58].

The first instance of utilizing the plant reduction method (using alfalfa extract) was carried out by Gardea-Torresdey in 1999 to produce face-centred cubic tetrahedrons, icosahedral polytwins, hexagonal sheets, decahedron polytwins, and unevenly shaped AuNPs. Recently,

the biological synthesis of valuable metallic nanomaterials such as silver and gold has emerged as a hot topic in the field of nanotechnology. Furthermore, since the reducing agents are derived from plant based materials, or microorganisms like bacteria, fungi, and yeast, this bio-synthesized nanoparticles production appears to pose a less detrimental to the environment; thus, it is a green synthesis approach has now emerged as a significant synthetic technique. Moreover, natural chemicals derived from plant based materials or microbes are used as precursors to reduce the metallic salt. In comparison to the physical method of synthesis of nanoparticles, biological synthesis of raw materials is economical, uncomplicated, eco-friendly, and simple to expand to obtain higher yields [59].

While there has been a lot of research on testing and evaluating plants to produce metallic nanoparticles, there has been relatively less scientific focus on the fundamental principles involved in synthesizing nanomaterials. Nanoparticles synthesis involves a variety of tools, materials and steps, including capping agents, reducing agents, growth, solvents, metal salts, nucleation, stabilization, aggregation, and characterization. The process typically relies on chemical reduction, which employs highly reactive agents like aldehydes, citric acid, tartaric acids amino acids, NADP reductase, flavonoids, and other secondary metabolites. In a report by two researchers, it was stated that the reduction potential of metals varies and has a significant impact on the reduction of metals or their precursors during synthesis. A higher positive reduction potential results in a faster reduction rate of the metal precursor. On the other hand, if the reduction rate is slow, the nucleation and growth phases are more likely to reach a state of equilibrium. [60].

Green synthesis is considered to be a promising mechanism for nanoparticles synthesis due to the use of non-hazardous and cost-effective input materials. Furthermore, this method of NP synthesis is feasible with elevated medicinal efficiency, low cytotoxicity, site-specific delivery, and targeted binding. Besides that, these nanoparticles have very less negative consequences for the environment or human health. Due to its affordability, utilizing plant-based green synthesis is a favourable choice for producing AuNPs on a large scale with precise size and shape. Compared to microorganisms such as fungi and bacteria, plants are a preferred option for NP synthesis since they exhibit the requirement of complex procedures involved in maintenance of microbial cultures [61].

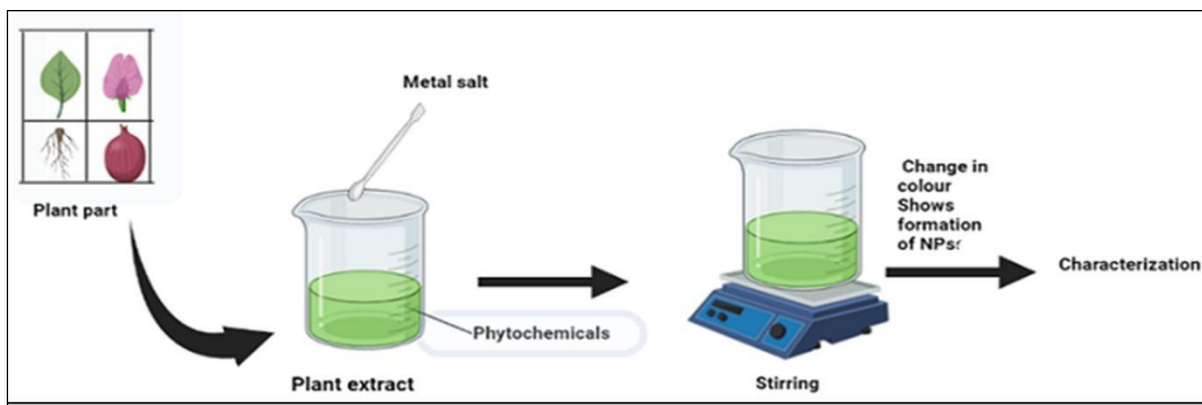


Fig 3: Green synthesis of nanoparticles using plant extracts

2.11 Gold Nanoparticles

The utilization of gold nanoparticles (AuNPs) has been extensive in the area of biotechnology at a nano scale because of their distinctive characteristics and different surface features. The ease with which AuNPs can be customized to have different functions makes them a versatile option for combining with antibodies, proteins, and oligonucleotides in nanobiological assemblies. Bioconjugates of AuNPs have also shown potential as promising biomaterials for investigating biological systems [62].

Gold nanoparticles are evolving materials with electrical and optical properties distinct from bulk materials and show considerable applications for use in medicine. Special characteristics of AuNPs involve surface chemistry, multi-functionalization, and surface Plasmon resonance, high surface area to volume ratio, and stable nature. AuNPs have the advantage of being easily manipulated into various sizes and shapes by varying the concentrations and components [63].

AuNPs can be shaped into spheres, rods, cages, and other morphology by both industrial and experimental formulation. The majority of research on AuNPs has focused on their bioconjugation with various biological molecules such as genes, drugs, peptides, and other specific target ligands. The antibacterial or antiviral activity of AuNPs conjugated with drugs or antibiotics is better compared to that of the antibiotics or drugs alone. According to the evidence, bare AuNPs have limited impact on bacterial growth and lack effective functional activity, whereas AuNPs combined with biomolecules hinder bacterial cell growth [64].

Gold nanoparticles are inert and thus offer less toxicity to living tissues. Thus, their functionalization is easy to deliver a feasible antibacterial activity against gram (-) ve, gram (+) ve as well as pathogenic bacteria [65].

Gold nanoparticles can bind to the bacterial membrane electrostatically and may interact vigorously with lysine residues present in the cell membrane of gram (+) ve bacteria, causing

irreversible pores to form and thus leading to the death of bacteria. Furthermore, once gold nanoparticles enter bacterial membranes they tend to reduce the generation of adenosine triphosphate (ATP), resulting in a declining metabolism rate. AuNPs encourage the photocatalytic performance of oxides like zinc oxide and titanium dioxide which causes to the production of hydroxyl groups, peroxides, and enhanced oxygen concentrations. This yields excess Reactive Oxygen Species (ROS) and starts causing bacterial cells to collapse. Gold nanoparticles have outstanding photothermal consequences when they are exposed to near-infrared light (NIR). The bacterial population is significantly suppressed when temperatures rise above 50 °C due to the denaturation of proteins [66].

The production of AuNPs using chemical synthesis is a frequently employed technique; it involves a reductant, a stabilizer and a metal precursor. Moreover, this method is not an assessment of biological activity as it involves the production of toxic byproducts during the synthesis period and functionalization of AuNPs, which may interfere with downstream testing methods. So as consequence, biological ('green') synthesis techniques are now available for the synthesis of AuNPs and have become more popular rather than other methods of synthesis in recent years. These strategies require the use of plant extracts, microorganisms, or extracellular or intracellular fungi or bacteria extracts. These techniques are typically inexpensive and simple, enabling the manufacturing of AuNPs on a large industrial scale [64].

2.12 Toxicity of gold Nanoparticles

AuNPs themselves are not hazardous; however, in a solution, they may become toxic due to the effect of capping agents and/or chemicals. The toxicity of AuNPs is also affected by parameters such as concentration, quantity, shape, and size. In fact, smaller nanoparticles ranging from 2 to 20nm appear to be more harmful than bigger nanoparticles due to their capacity to concentrate more quickly in the liver and spleen because of their superior circulation time and bio-distribution. Toxicity may also be dependent on the mode of synthesis involved for the generation of nanoparticles. Green synthesis methods should be employed to reduce the toxicity of gold nanoparticles. Furthermore, the rapid accumulation of AuNPs in the spleen and liver and the kind of functional molecules they have, contribute to the AuNPs toxicity rate [68].

Infections caused by microbes pose a wide range of diseases which are long lasting and persistent and kill approximately 10 million people each year, the majority of whom live in tropical countries. Because of their low cost and potency, antibiotics have been used to treat

bacterial infections. But abuse and overuse of these antibiotic drugs, have aided in the spread and development of mechanisms of resistance among bacteria, likely to result in the development of multiple drug-resistant (MDR) microorganisms. In the United States, the annual cost has been estimated to rise by \$20 billion because of multidrug-resistant (MDR) microorganisms [69, 70].

2.13 Role of Nanoparticles in Biofilm inhibition

If nanoparticles are co-incubated or either in close proximity with biofilm, they can be altered to selectively target and combat one or multiple types of bacteria. The interaction between nanoparticles and biofilm involves three important steps. First, the nanoparticles approach the biofilm surface from the bulk phase and interact with it. The nature of this interaction is dependent upon the nanoparticles' chemistry of surface, charge, and hydrophobicity, which determine whether they interact with proteins, lipopolysaccharides, or lipids found in the cell membrane of the bacterial. As a result of this interaction, nanoparticles are able to infiltrate the biofilm. The extent to which the nanoparticles are able to penetrate depends on several factors, including the maturity of the biofilm, the composition and chemistry of its surface, the size of the nanoparticles, their surface charge and chemistry, as well as their concentration. Following their infiltration, nanoparticles may migrate internally as intact particles or as metallic ions such as silver ions (Ag^+) and ions (Au^+) that have leached from the nanoparticles. This migration allows the nanoparticles to interact with various components of the biofilm and bacterial cells, which contributes to their antimicrobial effects. Specifically, gold and silver nanoparticles disrupt several components of the biofilm and bacterial cells, making them effective against a range of bacterial species. During the process of approaching the biofilm surface, different types of interactions take place, such as the penetration and internal migration of nanoparticles. These interactions are typically regulated by a blend of attraction forces, including electrostatic interactions, hydrophobic interactions, hydrogen bonding and Van der Waals interactions [71].

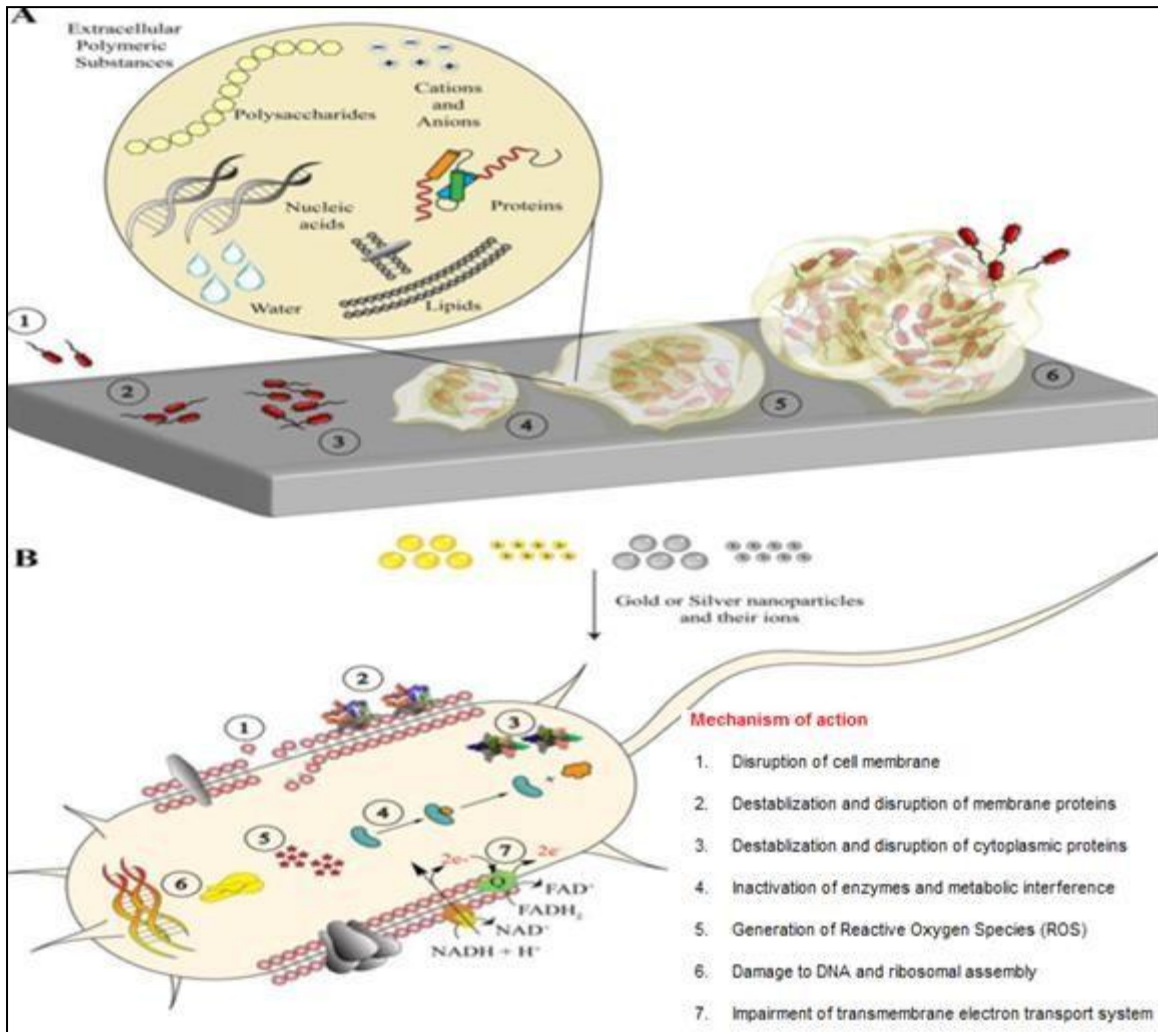


Fig 4: Mechanism of nanoparticles to inhibit biofilm [71]

2.14 *Withania somnifera*

W. somnifera belongs to the Solanaceae family, it is an evergreen woody, xerophytic, tender, and short perineal shrub that rise up to 2m in height and 1 m in width. This plant owns tomentose branches having silver-grey coloured fine short hairs that are outspread from the principal stem. The stems can be prostrate or erect and appear to be brownish in colour. Alternate phyllotaxy of leaves with very few hairs and greenish from the top while ample amount of hairs is present on the downside. This plant is characterized by dull, green elliptic, simple, glabrous leaves and small, bell-shaped green flowers. Leaf nodes have approximately 1-7 very small bisexual flowers with 5 yellow-orange stamens protruding out. Fruit is hairless, 5-8mm in diameter kept swollen, and membranous persistent calyx appears to be

red-orange when matured. Roots are fleshy, and stout, having fibre-like secondary branches arising from a central root with a bitter, arid taste and a strong odour [72].

It is an ayurvedic herb that has been renowned since antiquity for its multiple benefits for health. It has been utilized in energy elevation, stress management, and reducing inflammation, anxiety, cortisol, depression, and blood sugar level. So far, the plant has exhibited various therapeutic properties, including anti-diabetic, anti-depressant, anti-epileptic, antipyretic, anti-coagulant, anti-arthritic, anti-oxidant, and anti-diabetic effects. Additionally, it has demonstrated palliative effects such as analgesic, rejuvenating, regenerative, and growth-elevating effects [73].

Saxena et al give an account for the presence of many pharmacologically important constituents in roots of WS such as starch alkaloids, reducing sugars, steroids, volatile oils, amino acids, glycosides, dulcitol, hentriacotane, and withaniol. Phenolic acid and flavonoids are important constituents that offer therapeutic activities like antioxidant properties. This may be due to the presence of phenolic acids, ascorbic acids, anthocyanins, tannins, flavonoids, and steroidal lactones [74].

2.15 Characterization of Nanoparticles

2.15.1 UV-Visible (UV-Vis) spectroscopy

Ultraviolet-Visible (UV-Vis) spectroscopy is a principal technique that is most commonly utilized to analyze the optical characteristics of gold nanoparticles. This technique tends to measure either absorption or transmission of light by the nanoparticles as a function of wavelength when illuminated by ultraviolet and visible regions of the electromagnetic spectrum. The results are provided in the form of a spectrum that provides information about the shape, size, and SPR (surface Plasmon resonance) properties of the AuNPs.

The surface plasmon resonance can be described as a reciprocal oscillation of the unbound electrons that exist on the surface of the nanoparticles; it occurs at a specific wavelength and is influenced by the shape, size, and type of nanoparticles to be analyzed. SPR is the reason for strong absorption as well as a scattering of light by the nanoparticles, thus it is an essential optical characteristic to study. The intensity and position of the SPR peak provided by UV-Vis spectroscopy are utilized to estimate the shape and size of the nanoparticles, and also it can provide rough details about the concentration of nanoparticles in a solution. Spectra can also provide little knowledge about the surface chemistry of particles. Aggregation and

change in the surface chemistry of nanoparticles are indicated by variations in the position and intensity of the SPR peak [75].

This is a non-invasive technique, which does not affect the integrity of the sample, and is also inexpensive as it does not require complex procedures for sample preparation. Major drawback of this technique is that the adsorption spectrum is easily influenced by pH, solvent, high electrolyte concentration, and temperature. Besides this, UV-Vis spectroscopy alone is able to gather very few information about bio-molecular structure [76].

2.15.2 Dynamic Light scattering

Dynamic light scattering (DLS) is another effective method for the characterization of nanoparticles that are widely utilized. This technique involves measuring the scattered light intensity and time dependence from a suspension of nanoparticles, which provides valuable data on the particle size-dependent Brownian motion, distribution of size, and stability of the nanoparticles in the solution.

The instrumentation involves the laser beam which is directed towards a solution having nanoparticles, and a detector is placed at a fixed angle to detect the scattered light. The light which is been scattered is then examined to ascertain the distribution of size of the nanoparticles present within the sample, while the self-correlation function of the scattered light provides details about the Brownian motion of the nanoparticles.

To accurately determine the hydrodynamic particle size (R_h) through DLS, several parameters such as solvent viscosity, temperature, and solvent refractive index should be predetermined. These parameters may significantly affect the results, thus careful consideration is necessary for accurate results.

DLS is a suitable method for quickly screening samples with polydispersity or for evaluating the quality of samples with relatively low dispersity [77].

2.15.3 Zeta potential

Zeta potential of nanoparticles can be defined as the difference in the electric potential of the surface of the particle and the solution in which they are dispersed. The stability of nanoparticles is an important parameter to be analyzed and this can be assessed by knowing the zeta potential of nanoparticles in solution. It gives an account of electrostatic attraction and repulsion among particles, if zeta potential is high it indicates stability as the electrostatic

repulsion between particles will be repelled and thus no agglomeration or aggregation will occur. The Zeta potential of nanoparticles could be examined by using an approach known as electrophoretic mobility. This technique includes the determination of the velocity of particles and how their motion is influenced whenever an electric field from outside is applied to the solution containing nanoparticles. Smoluchowski equation can be utilized to determine the zeta potential using the data provided for the velocity of particles, as velocity is directly linked to zeta potential. Usually, colloids that are found to have zeta potential values ranging from ± 20 -30 mV or above are deemed to be stable [78].

2.15.4 X-Ray Diffraction

X-ray diffraction (XRD) is a commonly utilized procedure for the analysis of nanoparticles. It provides valuable knowledge about the crystalline structure, lattice parameters, nature of phase, and the size of crystalline grains. The Scherrer equation is used to estimate the size of crystalline grains by analyzing the broadening of the most intense peak in an XRD measurement of a specific sample. XRD offers the advantage that it can be performed on powdered samples, which are usually obtained by drying their corresponding colloidal solutions. One limitation of X-ray diffraction is its unsuitability for analyzing amorphous materials. Additionally, the technique may not be effective for particles smaller than 3 nm as the resulting XRD peaks may be overly broad [78].

X-ray diffraction has an edge over other analysis methods because it is non-destructive and requires minimal sample preparation. Powder X-ray diffraction (PXRD) is a non-invasive and rapid technique used for identifying solid phases. The unique X-ray powder pattern of each crystalline form of a compound makes it possible to identify the compound accurately. Furthermore, PXRD is a non-destructive method [79].

2.15.5 Fourier Transform Infrared spectroscopy

Fourier transform infrared spectroscopy is a method that involves measuring the absorption of electromagnetic radiation in the mid-infrared region (4000 - 400 cm^{-1}) to analyze molecules. When a molecule absorbs IR radiation, its dipole moment is altered, rendering it IR active. The resulting spectrum identifies the position of bands corresponding to the nature and intensity of bonds, as well as specific functional groups. This data provides valuable insight into molecular structures and interactions [78].

FTIR spectroscopy primarily focuses on non-aqueous samples due to the challenge posed by the strong absorption bands of water in aqueous systems. In addition, this technique enables the study of molecular conformations, bonding types, and functional groups at the molecular level. Vibrational spectra exhibit molecule-specific spectral bands, thereby providing direct information on the biochemical composition [78].

2.15.6 Scanning electron Microscopy

It is one of the high-resolution microscopy techniques that can provide a lot of information about the morphology of nanomaterial by using a concentrated beam of electrons falling on the sample at an ultra-fine scale. This technique can comprehensively monitor the size, formation, size distribution, and formation of synthesized micro and nanosized particles on their surface. SEM can also provide specific information related to the purity and extent of particle aggregation in a sample. One drawback of SEM is that it cannot provide information about the internal structure of the sample being analyzed [80].

SEM characterization involves a highly concentrated beam of electrons that is used to scan the surface of a sample. In the case of nanoparticles, a typical preparation technique involves placing the dispersed particles onto a TEM grid. By detecting secondary electrons, SEM is capable of providing valuable data regarding the shape and morphology of the nanoparticles [81].

2.15.7 Transmission electron microscopy

Transmission electron microscopy (TEM) allows an electron beam to pass through a thin sample, providing accurate data about the sample's internal structure. It is a powerful imaging technique that has found extensive application in nanomedical research, as it can offer valuable insights into the intricate connections between nanoparticles and cell or tissue components, thanks to its exceptional resolution [82]. High-resolution transmission electron microscopy (HRTEM) is a mode of TEM imaging that enables the observation of a sample's crystallographic structure at the atomic level. This technique is particularly useful for investigating nanoscale properties of crystalline materials, as it provides high-resolution imaging capabilities that can detect individual atoms and crystalline defects. When the electron beam interacts with the atomic columns of a crystalline specimen at high magnifications, phase contrast occurs, resulting in different contrast mechanisms. This effect can be utilized to image atomic distances in properly oriented crystals and provides valuable

information on crystal lattice distances and interface details with sub-nanometre precision. Overall, HRTEM is a powerful technique that can enhance our understanding of the atomic structure of materials [83].

CHAPTER 3
MATERIALS AND METHODS

3.1 Materials

3.1.1 Bacterial strains

Table 2: List of microbes used in study

<i>E. coli</i> DHα	Institute of Microbial Technology (IMTECH), Chandigarh, India
<i>M. smegmatis</i> MC ² 155	Central Drug Research Institute (CDRI), Lucknow, India

3.1.2 Media and other Chemicals

Table 3: List of Chemicals

Crystal Violet	Loba Chemie
Grams Iodine	Loba Chemie
95% Alcohol	Analytical grade
Safranin	Loba Chemie
Basic fuschin	Merk
Methylene Blue	Fisher scientific
Sodium Hydroxide pellets	Merk
Gold (III) Chloride	Sigma-Aldrich
Aluminium foil	BIO-MATRIX
Antibiotic discs of Gentamycin	HIMEDIA
Whatman filter paper	Cytiva
Milli Q water	Elix

3.1.3 Instruments used

Table 4: List of Instruments

Centrifuge	Eppendorf
4°C storage	BLUE-STAR
Incubator shaker	Labnet
UV-VIS spectrophotometer	Thermo Scientific
Water bath Sonicator	SONIX

3.2 Methods

3.2.1 Different streaking methods

Simple streaking

1. The petri plate was labelled with the name of the microorganism, and date.
2. The inoculation loop was sterilized by holding it on the flame of a Bunsen burner until it became red hot.
3. The loop was cooled by placing it on the corner of a sterile nutrient agar plate.
4. The bacterial culture was grasped while holding the loop by one hand, and the cotton plug was removed using the ring finger and little finger.
5. The mouth of the flask was heat sterilized by keeping it in front of the burner for 5-10 seconds.
6. The loop was inserted into the broth culture and picked up a film.
7. The cotton plug was again fixed on the mouth of the test tube.
8. The loop was dragged gently on the nutrient agar plate in a zig-zag pattern.
9. The loop was again sterilized until it became red hot.
10. The plates were kept inverted in an incubator for 24 hours at 37°C.

Quadrant streaking

1. The loop was sterilized by holding it in a blue flame and allowed to cool.
2. A loop full of culture was placed on the agar surface.
3. A smear was prepared at one extreme end and the loop was dragged back and forth across the agar surface.
4. The loop was sterilized again.
5. The plate was rotated 90 degrees and other streaks were made from the end of the previous streak.
6. The same process was repeated two more times.

7. The plate was incubated overnight at 37°C for 24 hours.

3.2.2 Gram Staining

1. Clean glass slide was taken and washed using detergent.
2. Wiped it using muslin cloth not by cotton as cotton fibres may stick to slide and give false results.
3. Smear of bacterial culture was prepared and few drops of normal saline were added.
4. Kept it for air drying and heat fix.
5. Added crystal violet (CV) drop wise and kept it for 1 minute.
6. Added few drops of grams iodine (mordant) for 1 min and again washed using distilled water.
7. Washed using 95% alcohol (decolourizer) for 20 sec and thereafter washed with distilled water.
8. Added few drops of safranin (counter stain) for 35 to 45 sec and again washed with distilled water.
9. Slides were air dried and observed under microscope.

3.2.3 Ziehl-Neelsen staining

1. A bacterial smear was made by taking 10 µL of broth culture on a sterile glass slide.
2. The smear was allowed to air dry and then heat-fixed.
3. The primary stain, 2-3 stain carbon fuschin, was added.
4. The stain was heated at 60°C until vapours began to rise, and allowed to remain on the slide for 5 minutes.
5. The stain was washed off with distilled water.
6. The smear was covered with acid-alcohol (decolourizer) for 5 min or until the smear was sufficiently decolorized to give a pale pink colour.
7. The slide was washed with clean water.
8. Counter-staining with Methylene blue or malachite green was poured for 1-2 min.
9. The slide was washed with clean water and blotted dry.
10. The slide was examined under a compound microscope

3.2.4 Preparation of plant extract of *Withania Somnifera*

1. Fresh leaves of *W. somnifera* were plucked and washed 2 times with tap water and once with distilled water.
2. Leaves were then dried in the oven at 40°C overnight.
3. Next day all leaves were ground using a mortar pestle and 1gm powder was added to 100ml Millipore water.
4. Obtained mixture was centrifuged at 7500rpm for 10 min and followed by filtration using Whatman filter paper (pore size 2mm)
5. The obtained extract was stored at 4°C, protocol for preparation and storage of plant extract was followed as described by Rao et al , 2018.[84]

3.2.5 Preparation of nanoparticles

3.2.5.1 Ratio optimization

1. pH of plant extract was set to 8 using 0.1 N NaOH
2. The plant extract was mixed with 1M HAuCl₄ solution in the different ratios given as follows:

Table 5: Different ratio of plant extract of *W. somnifera* and 1M HAuCl₄

Sample NO.	Plant extract (Reducing and capping agent)	1M HAuCl ₄ solution (Metal salt)
Sample 1	5mL	1mL
Sample 2	1mL	1mL
Sample3	2mL	3mL
Sample 4	3mL	2mL
Sample 5	7mL	1mL
Sample 6	9mL	1mL

3. Test tubes were covered with aluminium foil to avoid photo degradation.
4. All test tubes were incubated at 30 °C overnight with 100rpm shaking.
5. UV-Vis spectra of each sample were recorded and plotted on a graph.

3.2.5.2 pH optimization

1. Took 5 test tubes marked them as 4, 6, 8, 10, and 12, and added 2mL of plant extract in each.
2. pH of each sample is set as marked on it i.e. 4, 6, 8, 10, and 12 respectively.
3. Added 14 ml of 1M HAuCl₄ solution and cover with aluminium foil.
4. All test tubes were incubated at 30 °C overnight with 100rpm shaking.
5. UV-Vis spectra of each sample were recorded and plotted on a graph.

3.2.7 Temperature Optimization

1. Took 6 test tubes, marked 20, 30, 40, 50, 70, and 90, and added 2mL of plant extract.
2. pH of the plant extract was set to 8
3. Added 14 ml of 1M HAuCl₄ solution and covered with aluminium foil.
4. All test tubes were incubated at 20 °C, 30 °C, 40 °C, 50 °C, 70 °C and 90°C with 100rpm shaking until colour of solution changed from yellow to ruby red.
5. UV-Vis spectra of each sample were recorded and plotted on a graph.

3.2.5.3 Time Optimization

1. 2ml of plant extract with pH 8 was added to 14ml of 1M HAuCl₄ (1:7 ratio) in a wrapped test tube.
2. Test tube was kept at 30 °C at 100 rpm.
3. UV-Vis spectra was recorded every hour and plotted on a graph.

3.2.5.4 Antibacterial activity of synthesized nanoparticles against *E. coli* and *M. smegmatis*

1. *E. coli* culture was inoculated in Muller-Hinton broth and *M. smegmatis* was grown in LBGT and incubated at 37°C overnight.
2. Muller-Hinton agar plates were prepared and incubated.
3. The overnight-grown culture was compared with the McFarland solution and was further diluted 2 times to get the appropriate number of cells.
4. The diluted culture was spread using a sterile swab to get a proper bacterial lawn.
5. Wells were punched using a sterile well puncher of appropriate size and distance from each other.
6. 200 µL of nanoparticles solution was pipetted into two wells.

7. One of the well is filled with 200 μ L Millipore water (control).
8. 200 μ L Plant extract was also added to one well.
9. Middle well is filled with antibiotic.
10. The plates were incubated overnight at 37°C.
11. The diameter of the zone of inhibition was measured, and the results were interpreted.

3.2.6 MIC of Green synthesised Gold nanoparticles

1. The bacterial cultures were subcultured in Muller Hinton broth and incubated for 6-8 hours at 37°C.
2. The turbidity of the culture was adjusted to match 0.5 McFarland or OD₆₀₀ was adjusted to 0.8 (culture was supposed to have 10⁸ CFU/ml).
3. This culture was initially diluted 1:150 to get 5 x 10⁶ CFU/ml and further 1:2 diluted to obtain 5 x 10⁵ CFU/ml. This diluted culture was used further inoculation.
4. Components were added according to the figure 5.
5. The blank was set by adding 200 μ l of distilled water to wells A1, B3, C3.
6. A2, B2, and C2 were used to set negative control for plant extract by adding 100 μ l plant extract and 100 μ l media.
7. A3, B3, and C3 were set as a positive control in which 100 μ l of media (LB) and 100 μ l of diluted culture were added.
8. A4, B4, and C4 had 100 μ l of 10 mg/ml concentrated plant extract and 100 μ l of culture were added.
9. Two-fold dilutions were performed using plant extract and media, and then 100 μ l of culture was added to each well.
10. D1, E1, and F1 were used for media control in which 200 μ l of media was added.
11. D2, E2, and F2 were used to set negative control for AuNPs by adding 100 μ l AuNPs and 100 μ l media

12. D3, E3, F3 were set as positive control in which 100µl of media (LB) and 100µl of diluted culture were added

13. D4, E4, F4 had 100µl of 27µg/ml concentrated AuNPs and 100µl of culture.

14. Two-fold dilutions were performed using AuNPs and media, and then 100µl of culture was added to each well.

15. The G and H rows were used as antibiotic control by performing two-fold dilutions.

16. The lid was closed and sealed using parafilm. Plates were then incubated at 37°C overnight for *E. coli* and 96 hours for *M. smegmatis*.

17. The optical density of each well was recorded and compared

	1	2	3	4	5	6	7	8	9	10	11	12
A	Blank(200µL water)											
B												
C		-ve Control(100µl plant extract+ 100µl media)	+ve Control (100µl media +100 µl culture)	5mg/ml PE + 100µL culture	2.5mg/ml PE + 100µL culture	1.25mg/ml PE + 100µL culture	0.62mg/ml PE + 100µL culture	0.31mg/ml PE + 100µL culture	0.07mg/ml PE + 100µL culture	0.03mg/ml PE + 100µL culture	0.01mg/ml PE + 100µL culture	0.009mg/ml PE + 100µL culture
D												
E	Media Control (200µL media)											
F		-ve Control(100µl AuNPs+ 100µl media)	+ve Control (100µl media +100 µl culture)	(127µg/ml +100 µl culture)	(63.5µg/ml +100 µl culture)	(31.75µg/ml +100 µl culture)	(15.8µg/ml +100 µl culture)	(7.93µg/ml +100 µl culture)	(3.96µg/ml +100 µl culture)	(1.98µg/ml +100 µl culture)	(0.99µg/ml +100 µl culture)	(0.47µg/ml +100 µl culture)
G												
H	1mg/ml cef +100µL culture	0.5mg/ml cef + 100µL culture	0.25mg/ml cef + 100µL culture	0.125mg/ml cef + 100µL culture	0.06mg/ml cef + 100µL culture	0.03mg/ml cef + 100µL culture	0.01mg/ml cef + 100µL culture	0.007mg/ml cef + 100µL culture	0.003mg/ml cef + 100µL culture	0.001mg/ml cef + 100µL culture	0.0009mg/ml cef + 100µL culture	0.0004mg/ml cef + 100µL culture

Fig 5: Microtiter plate depiction for MIC and antibiofilm assay

3.2.7 Biofilm assays

3.2.7.1 Growth of *E. coli* biofilm

1. *E. coli* was grown in Nutrient broth medium and *M. smegmatis* was grown in LBGT ,both were grown until they achieved an optical density of 0.4 at 600nm.
2. The culture was diluted 10 times using the same medium (Nutrient broth and LBGT) used for initial inoculation.
3. Components according to Figure 5 were added and 100 μ L of the diluted culture was used to inoculate the wells of a 96-well microtiter plate
4. The lid was covered, and the plate was incubated at 37°C for 24 hours for *E. coli* biofilms and 96 hours for *M. smegmatis* biofilms.

3.2.7.2 Crystal Violet Assay

1. The contents of wells were removed and collected in a collection jar.
2. The wells were washed two times using autoclaved distilled water.
3. The wells were blot dried by tapping the plate on blotting sheets.
4. 225 μ L of 1% Crystal Violet stain was added to each well having biofilm.
5. It was kept for 15 minutes at room temperature.
6. The wells were washed twice using 225 μ L of sterile water.
7. 200 μ L of 95% ethanol was added to solubilize biofilm.
8. The plate was stored at room temperature for 15 minutes and then the contents were swirled.
9. Optical density was recorded at 570, protocol for biofilm assay was followed as per described by Sharma et al., 2021 [85].

3.2.7.3 Colony forming unit (CFU) count method

1. The culture was removed and collected in a collection jar.
2. The wells were washed using 200 μ L of nutrient broth medium.
3. The wells were dried by gently tapping on a blotting sheet.

4. 100 μ L of nutrient broth medium was added to each well.
5. The attached biofilm was gently scraped from the well surface using a pipette tip.
6. The contents were collected in a microcentrifuge tube.
7. The microcentrifuge tube was sonicated in a water bath sonicator at 25°C and 40 kHz frequency.

Serial dilution and plating

1. Nutrient agar tween plates were prepared.
2. Dilutions were made of the sonicated mixture in tween normal saline
3. 100 μ L of the spread culture was plated on the agar.
4. CFUs of biofilm-forming cells were determined, protocol for biofilm assay was followed as per described by Sharma et al., 2021 [85].

CHAPTER 4

RESULTS

4.1 Streaking

4.1.1 Simple streaking

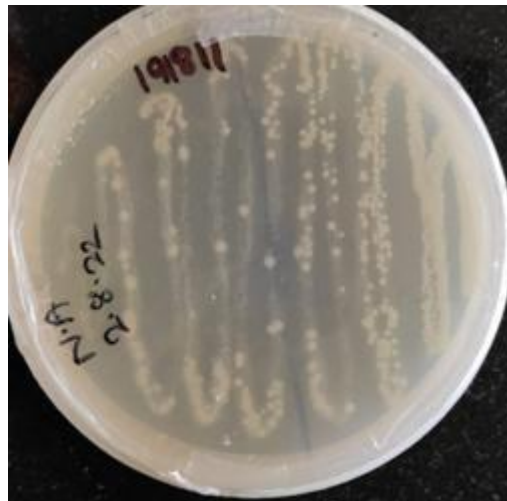


Fig 6: Simple streaking of *E. coli*

4.1.2 Quadrant streaking

To obtain isolated colonies of *E. coli* and *M. smegmatis* quadrant streaking was done. These colonies of both the organisms were obtained and used for further subculturing.



7(a)

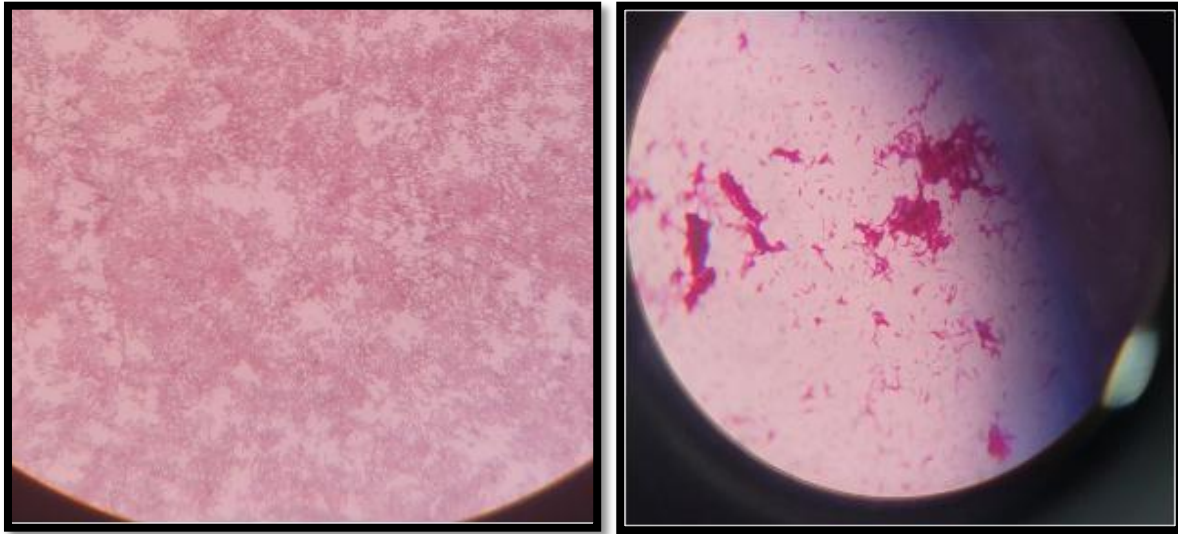


7(b)

Fig 7 (a): Quadrant streaking of *M. smegmatis*; 7 (b): Quadrant streaking of *E. coli*

4.2 Staining

Gram staining and Ziehl-Neelsen staining was done to confirm that the culture was free of contamination.



8(a)

8(b)

Fig 8(a): Gram staining of *E. coli*; 8(b): Ziehl- Neelsen staining of *M. smegmatis*.

4.3 Plant Extract Preparation



Fig 9: *W. somnifera* water extract obtained after drying and maceration.

4.4 Preparation of nanoparticles

The plant extract exhibited a brownish-red hue, whereas the HAuCl_4 solution appeared light yellow and transformed into reddish to slightly purplish colour after incubation. Colour change indicates formation of nanoparticles.

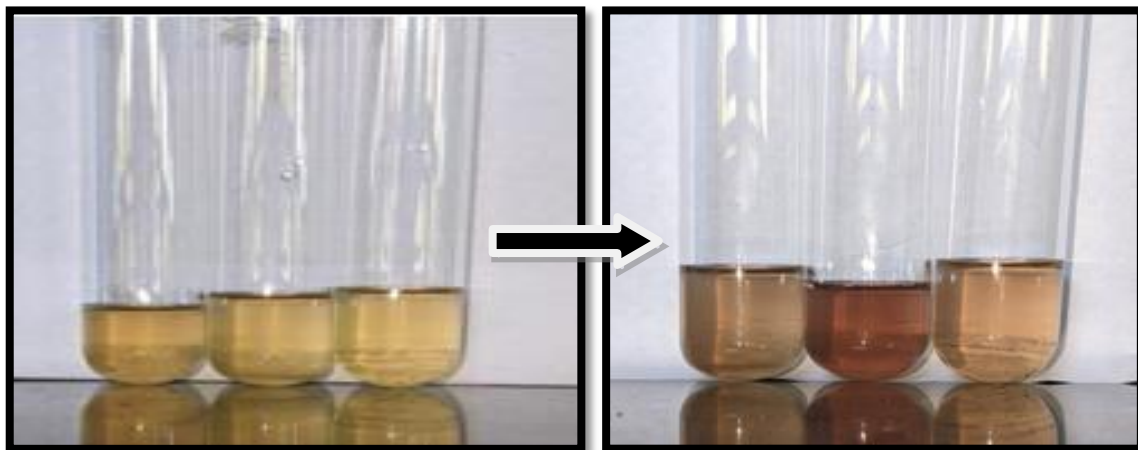


Fig 10: Colour of reaction mixture before and after 4 hours of incubation at 30°C.

4.4.1 Ratio Optimization

The UV-Vis spectra were analyzed for various ratios, and it was determined that the 7:1 sample exhibited the most suitable peak. A higher peak in the spectrum indicates a greater concentration of nanoparticles formed, while a narrower peak suggests that the nanoparticles are monodispersed.

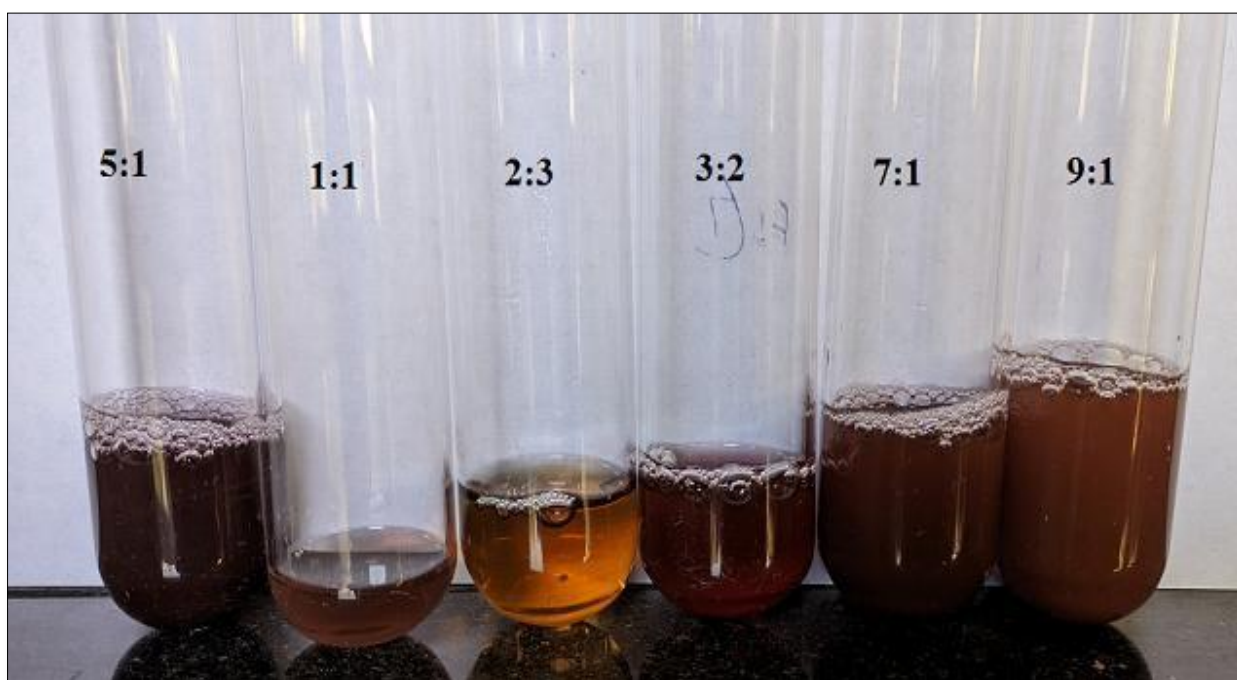


Fig 11: Colour change after 4 hours of different ratio

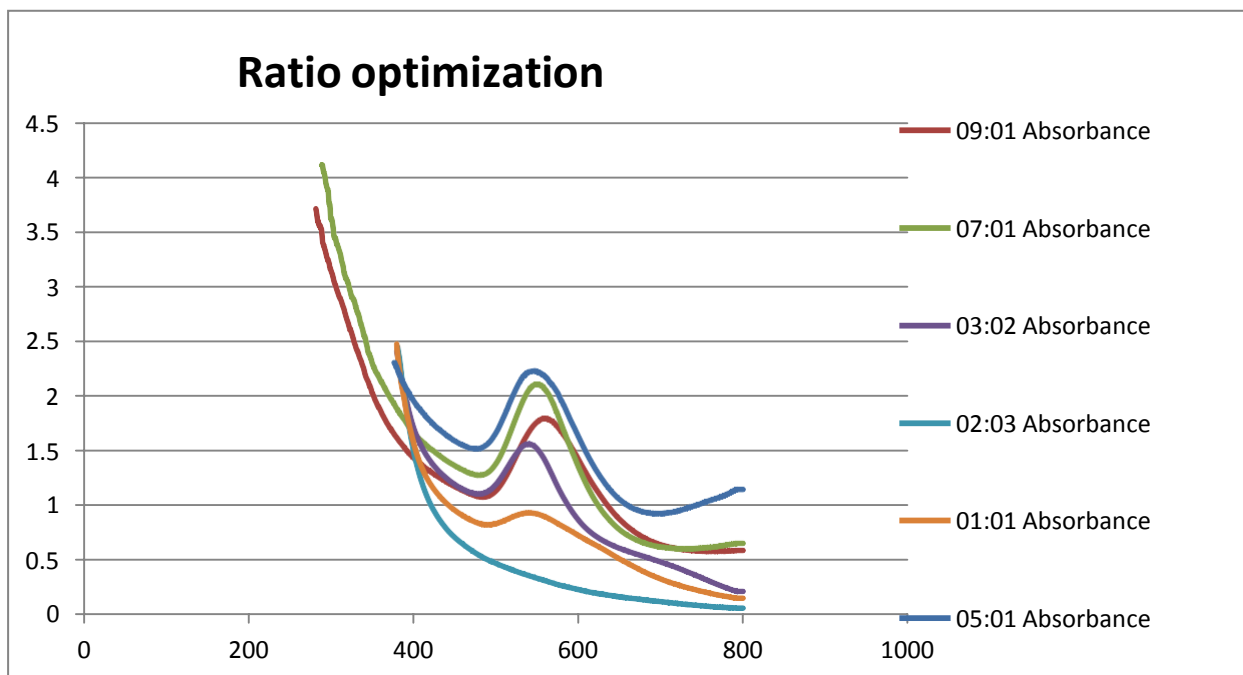


Fig 12: UV-Vis spectra of different samples for optimization of ratio of Plant extract and salt solution

4.4.2 pH optimization

The size of particles can be significantly influenced by pH. The pH level of HAuCl_4 was found to be 3.63, while the plant extract had a pH of 6.43. An examination of the UV-Vis spectra at various pH levels revealed that nanoparticles produced at a pH of 8 yielded favourable outcomes.

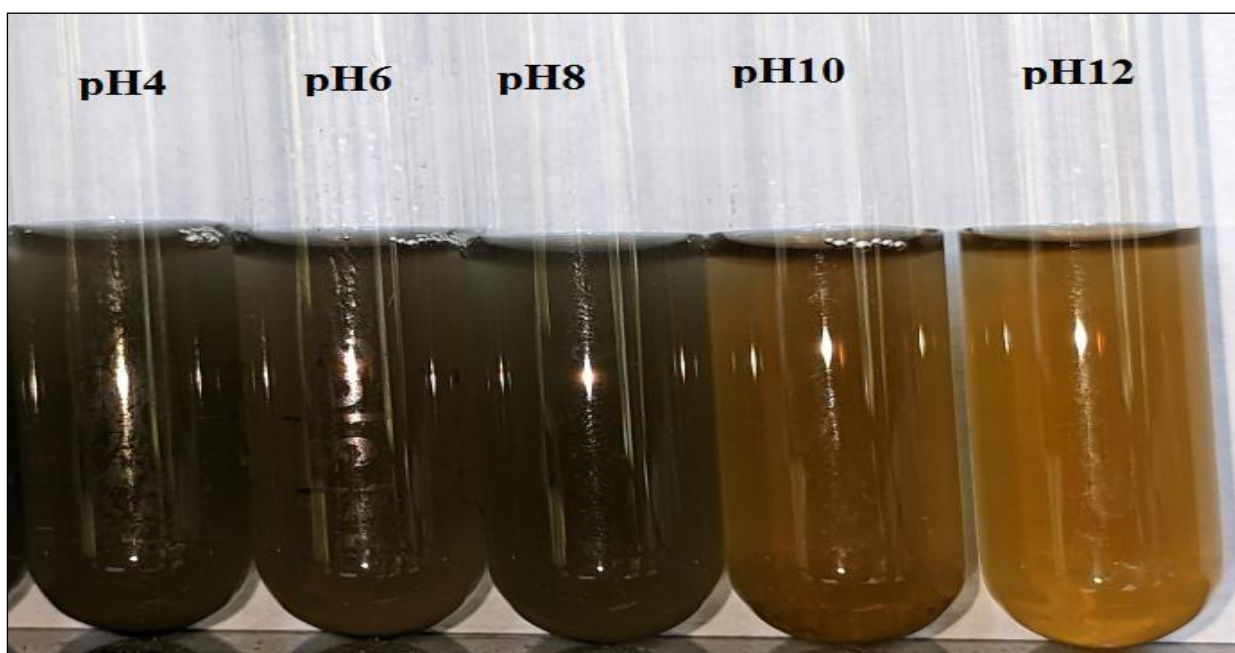


Fig 13: Colour change after 4 hours of different pH

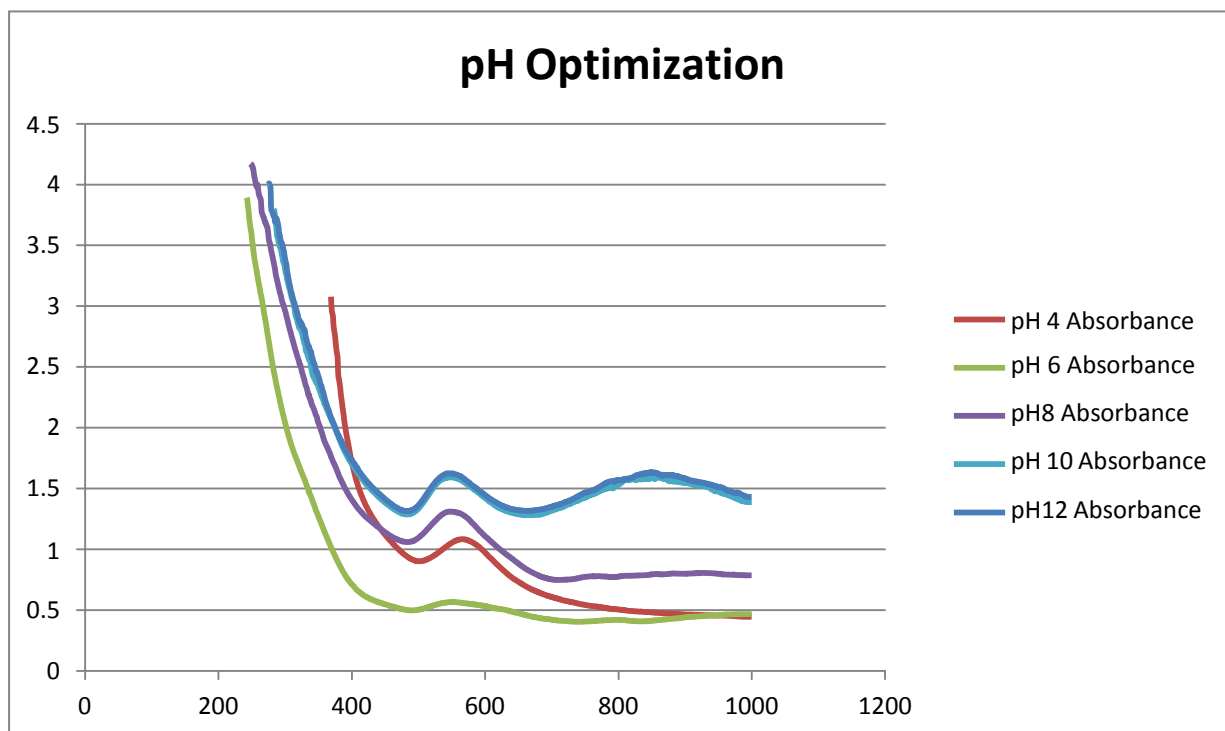


Fig 14: UV-Vis spectra of samples with different pH of plant extract

4.4.3 Temperature Optimization

Once the ratio and pH were optimized and held constant, the nanoparticles were incubated at various temperatures, and it was found that 30°C was the most favourable temperature. While an increase in temperature leads to a faster colour change, it also results in the production of less stable nanoparticles.

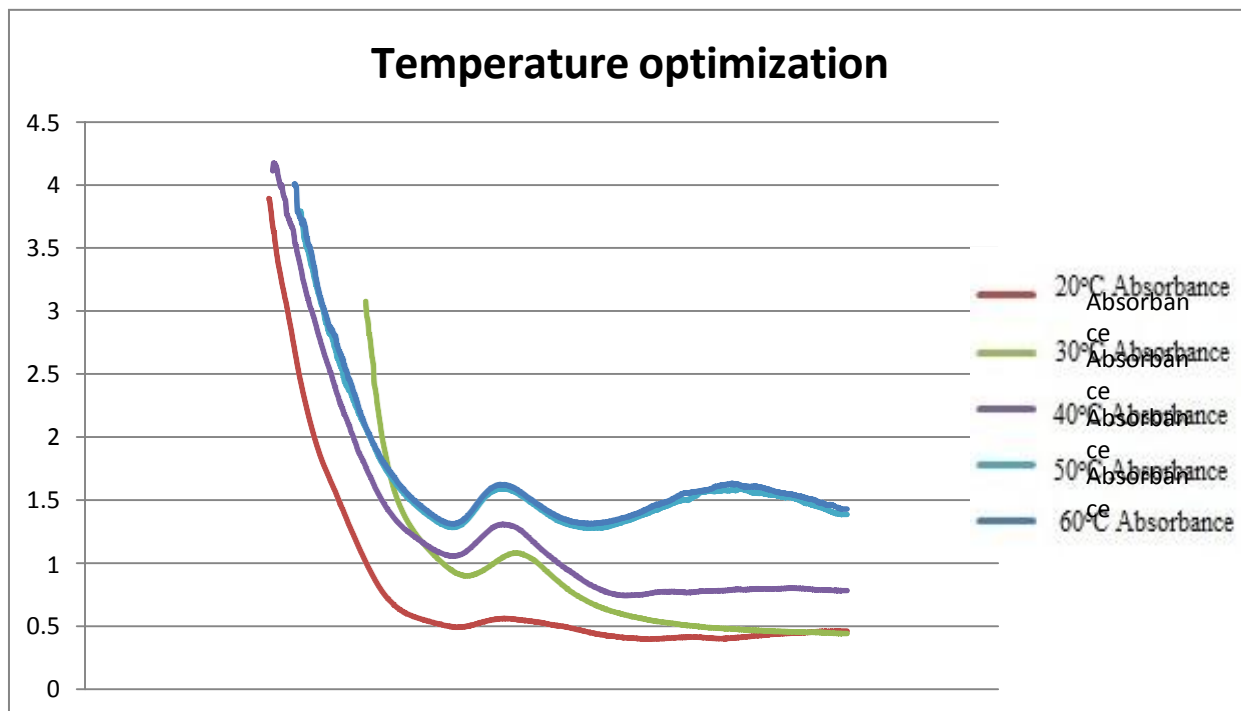


Fig 15: UV-Vis spectra of nanoparticles incubated at different temperature

4.4.4 Time optimization

After optimizing the nanoparticle's ratio, pH, and temperature, the incubation time for synthesis was also fine-tuned. Although a colour change was noticeable after 4 hours, the highest concentration was achieved after 10-11 hours. By examining the accompanying graph, it was determined that incubation time of 10 hours produces satisfactory results. Increasing the incubation time beyond this point does not lead to a significant increase in concentration of nanoparticles.

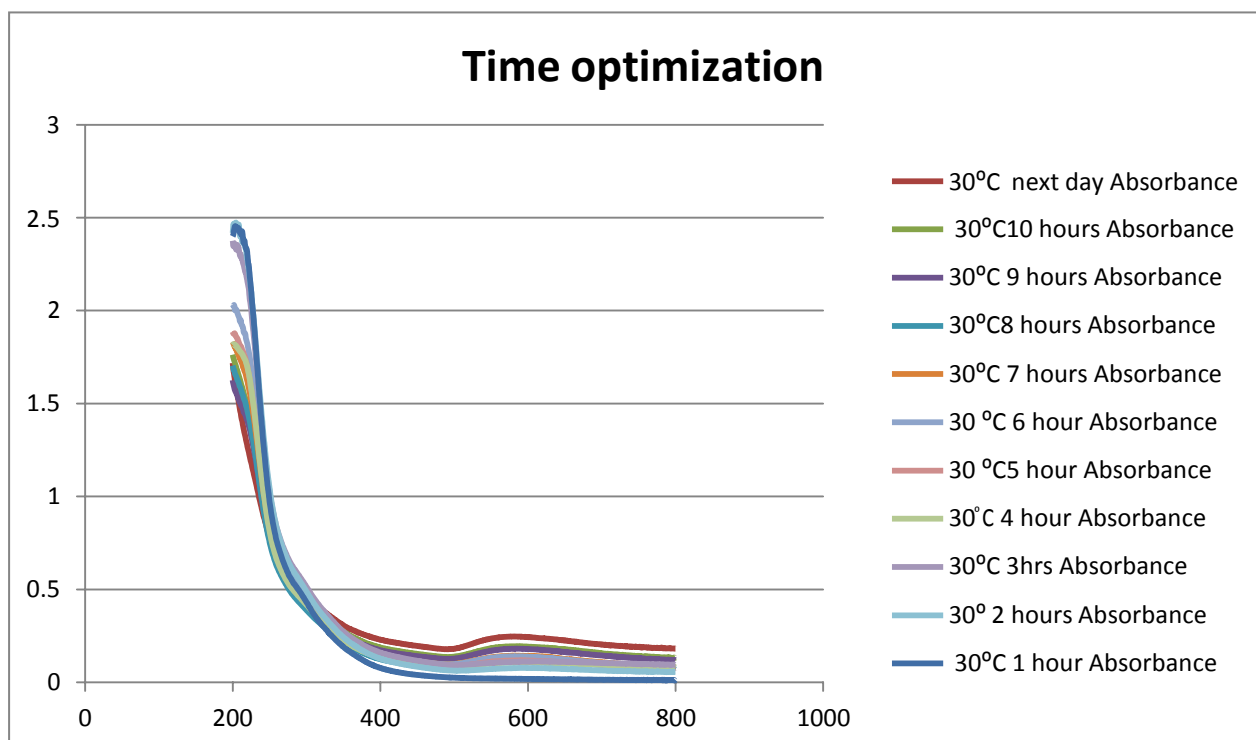


Fig 16: UV-Vis spectra of nanoparticles at different time period.

4.5 XRD result

Formed nanoparticles are crystalline in nature. XRD data showed that main peak is at 38.1 which corresponds to (111) plane and other peaks are at 44.3(200), 64.5(220), 77.5(311) when plotted on intensity v/s 2θ graph. This indicates face-centred cubic crystal character of gold nanoparticles.

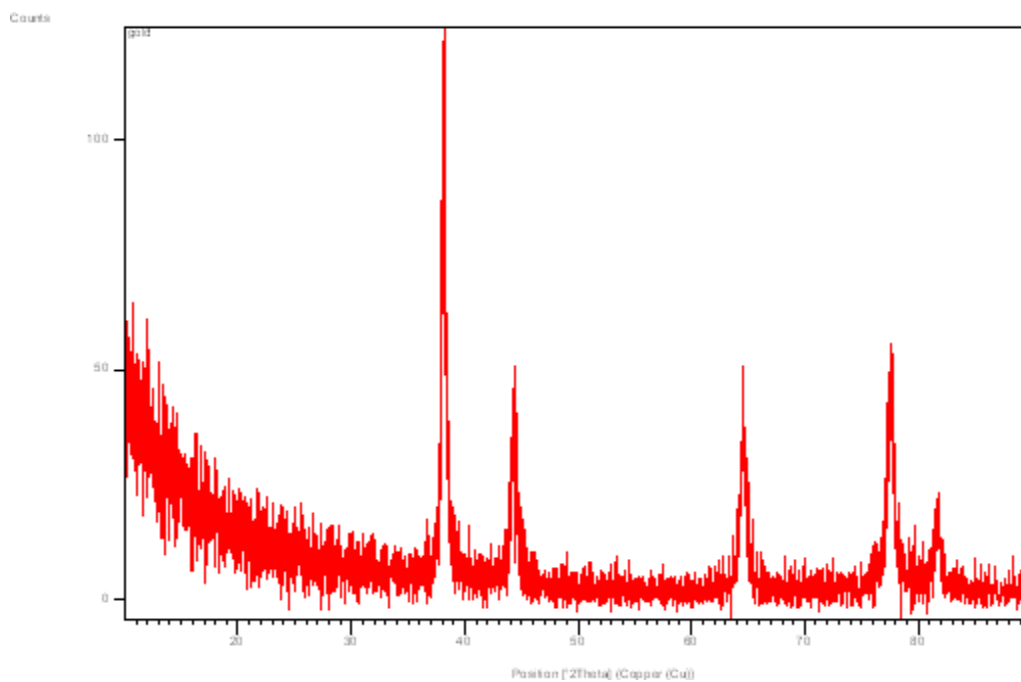


Fig 17: Intensity v/s 2degree Θ graph of XRD

Peak List

Pos.[$^{\circ}$ 2Th.]	Height[cts]	FWHM[$^{\circ}$ 2Th.]	d-spacing[\AA]	Rel.Int.[%]
38.1507	95.19	0.4498	2.35702	100.00
44.3500	33.06	0.6060	2.04087	34.74
64.5787	31.10	0.6337	1.44198	32.67
77.5469	38.04	0.6550	1.23003	39.96
81.6910	12.54	0.6524	1.17779	13.18

4.6 FTIR results

Gold nanoparticles are analyzed using Fourier transform infrared spectroscopy (FTIR), which involves studying the sample's absorption of infrared radiation.

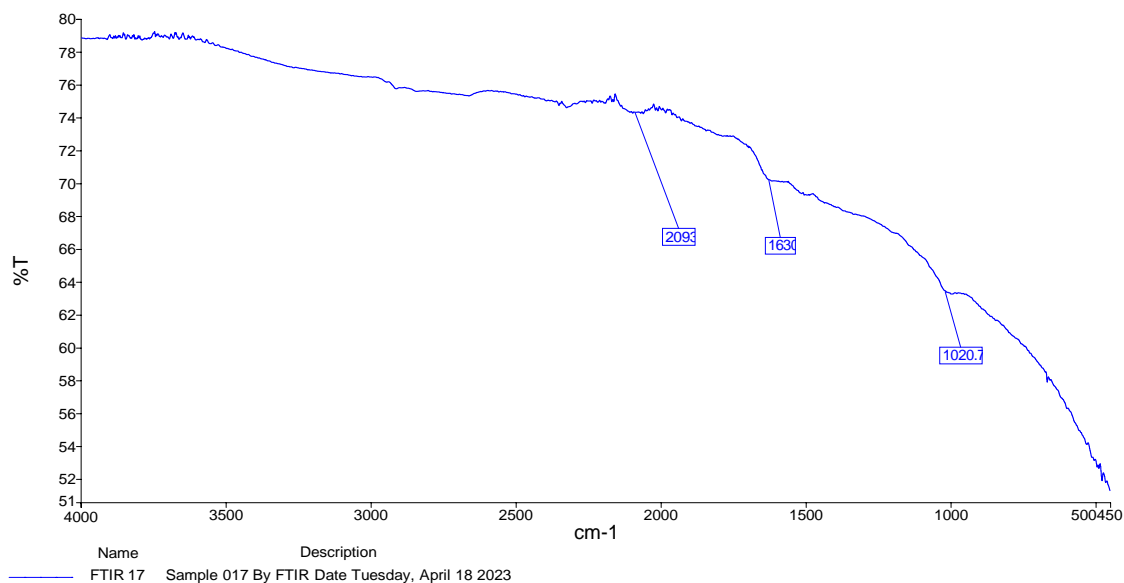


Fig 18 (a): FTIR analysis of powdered green synthesised gold nanoparticles.

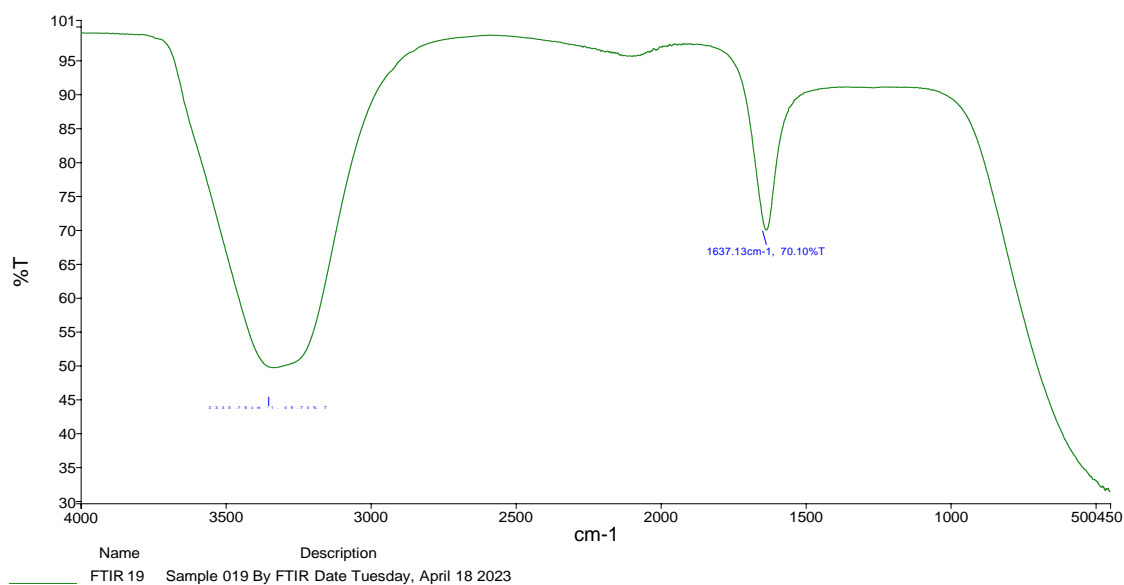


Fig 18 (b): FTIR analysis of suspended green synthesised gold nanoparticles.

Peak Number	X (cm-1)	Y (%T)
1	3340.76	49.74
2	1637.13	70.1

4.7 Dynamic Light Scattering

Hydrodynamic diameter of nanoparticles was found to be 151.85, Hydrodynamic diameter give an estimation of size which includes inorganic core coated with molecules/ ligands. Accurate size is measured by TEM.

Polydispersity Index was come out to be 17.11% which indicates that the size distribution of nanoparticles is narrow. PDI values between 10-30% are acceptable for gold nanoparticles.

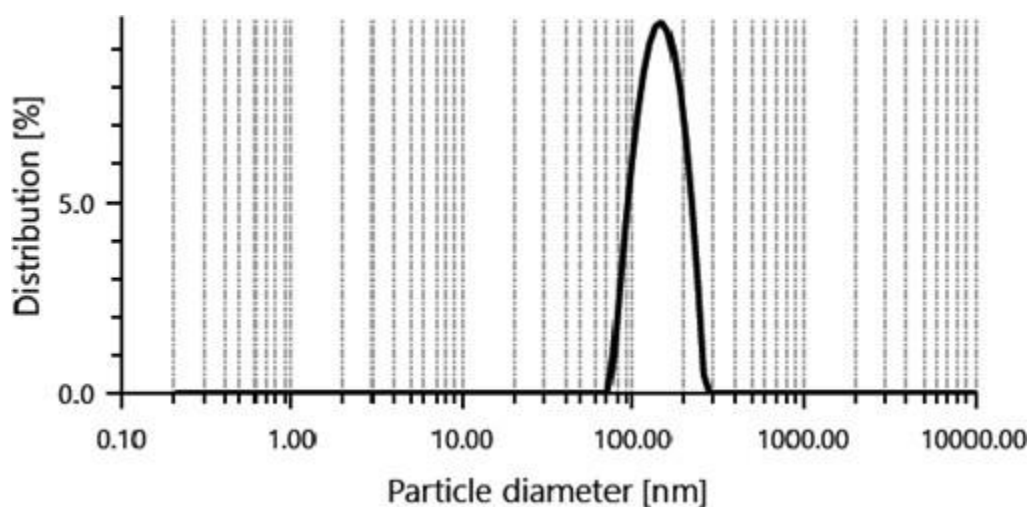


Fig 19(a): Particle diameter [nm] v/s distribution [%] graph of DLS

Hydrodynamic diameter= 151.85nm

4.8 Zeta potential

Zeta potential values of nanoparticles are found to be -23mV. Zeta potential values -30mV to +30mV are thought to be stable but negative values indicate high chances of aggregation.

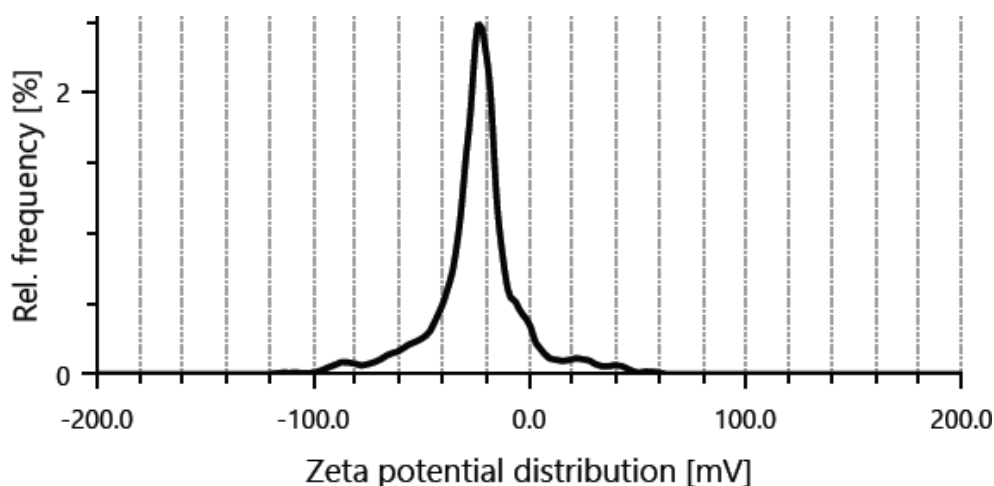


Fig 19(b): Zeta potential v/s relative frequency graph of Zeta potential analysis

Mean zeta potential= -23.4m

4.9 Antimicrobial Susceptibility Test

Antimicrobial susceptibility of nanoparticles were examined against *E.coli* and *M. smegmatis* using well diffusion method

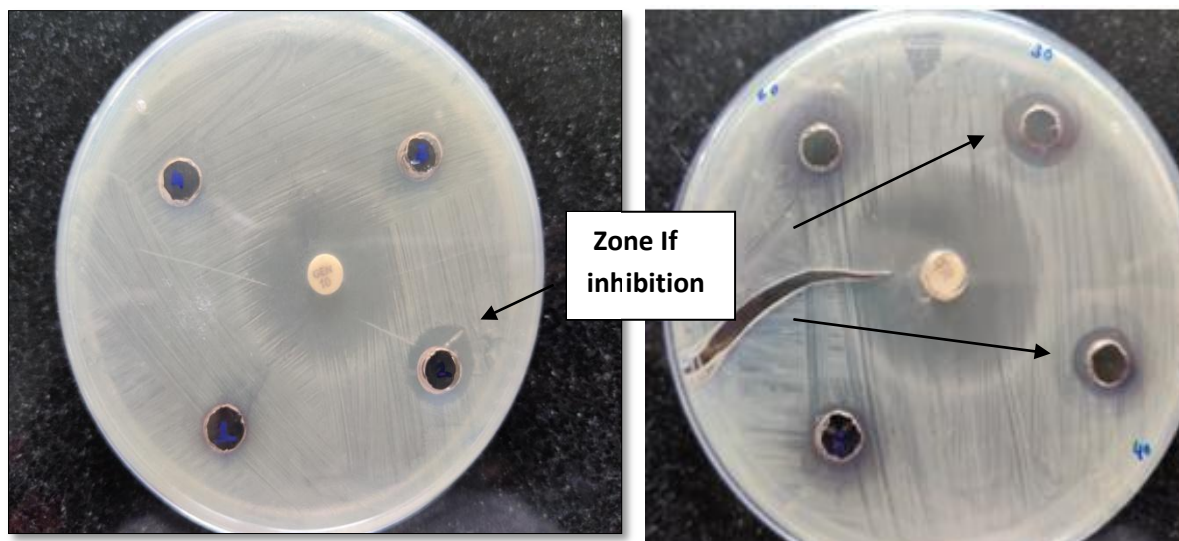


Fig 20: Zone of inhibition shown by green synthesised nanoparticles against *E. coli*

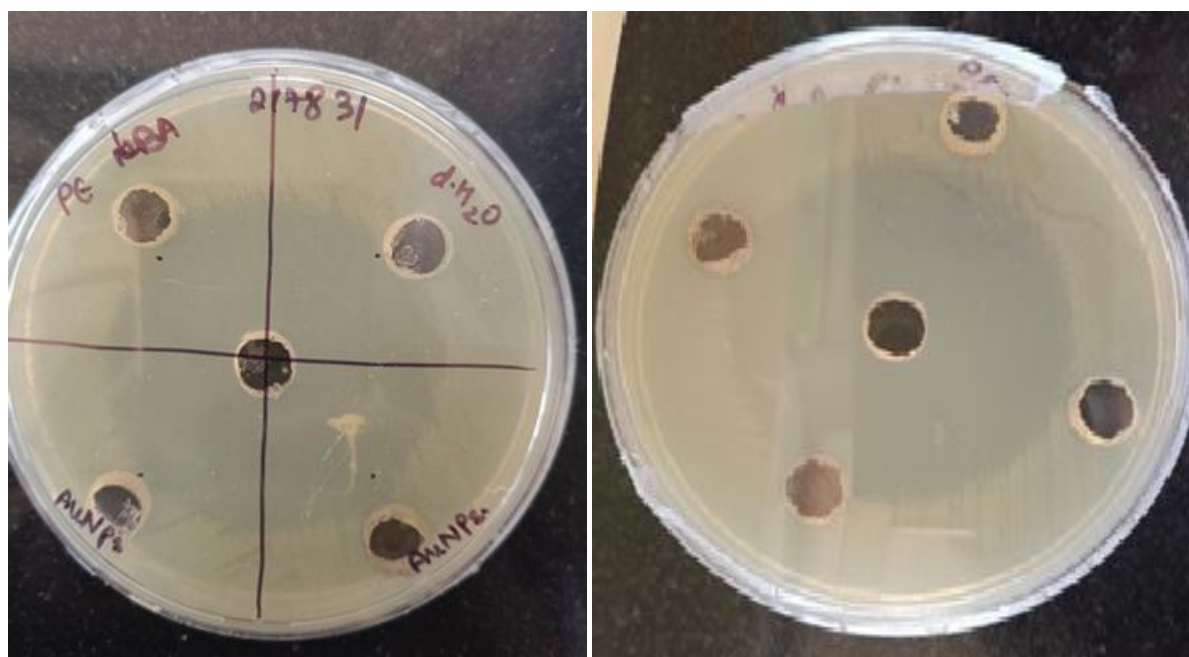


Fig 21: No zone of inhibition shown by green synthesised nanoparticles against *M. smegmatis*

4.10 MIC of nanoparticles against *E. coli*

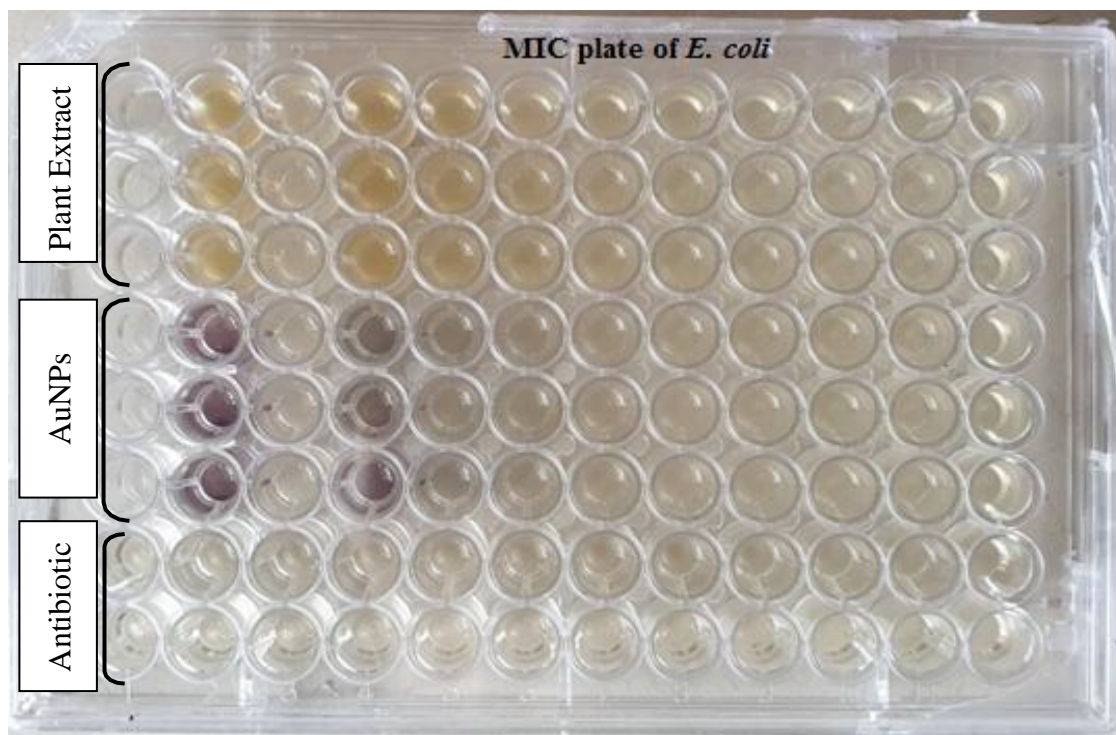


Fig 22: Microtiter well plate for testing MIC of *E. coli*

Table 5: OD₅₇₀ readings of *E. coli* to determine MIC

	1	2	3	4	5	6	7	8	9	10	11	12
A	0.000	0.250	0.432	0.283	0.359	0.331	0.341	0.347	0.330	0.356	0.438	0.342
B	0.000	0.230	0.422	0.350	0.334	0.328	0.338	0.362	0.343	0.339	0.339	0.378
C	0.000	0.236	0.399	0.343	0.321	0.340	0.329	0.355	0.335	0.353	0.355	0.373
D	0.042	0.400	0.321	0.520	0.349	0.304	0.307	0.326	0.323	0.330	0.367	0.322
E	0.047	0.503	0.385	0.546	0.305	0.323	0.303	0.318	0.422	0.396	0.427	0.595
F	0.046	0.450	0.351	0.768	0.353	0.326	0.379	0.313	0.362	0.519	0.425	0.490
G	0.010	0.010	0.017	0.017	0.017	0.016	0.020	0.025	0.027	0.032	0.036	0.045
H	0.009	0.011	0.018	0.0140	0.014	0.023	0.012	0.023	0.027	0.030	0.034	0.044

4.11 MIC of nanoparticles against *M. smegmatis*

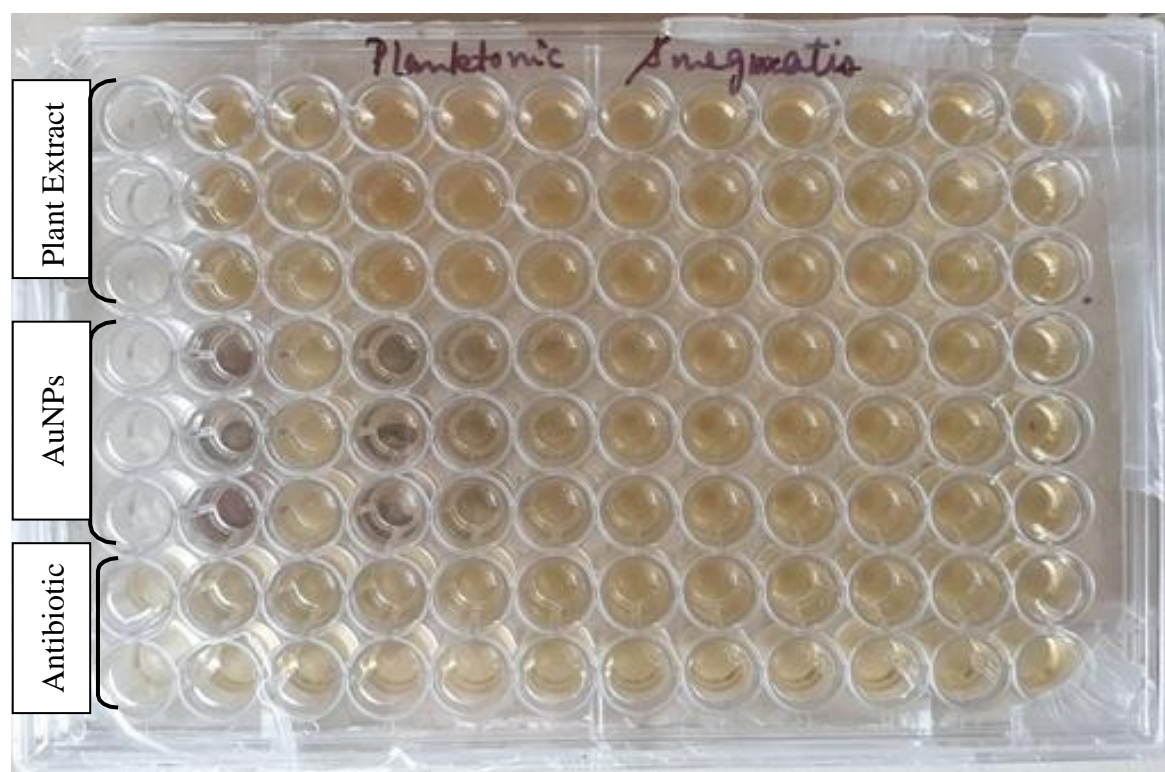


Fig 23: Microtiter well plate for testing MIC of *M. smegmatis*

Table 6: OD₅₇₀ readings of *M. smegmatis* to determine MIC

	1	2	3	4	5	6	7	8	9	10	11	12
A	0.000	0.209	0.064	0.275	0.246	0.136	0.093	0.080	0.058	0.1049	0.052	0.06
B	0.000	0.204	0.096	0.286	0.213	0.174	0.127	0.106	0.107	0.121	0.089	0.080
C	0.000	0.215	0.119	0.295	0.197	0.151	0.168	0.130	0.1778	0.138	0.145	0.056
D	0.004	0.243	0.107	0.290	0.202	0.146	0.198	0.147	0.1847	0.155	0.147	0.099
E	0.002	1.104	0.148	0.293	0.187	0.129	0.135	0.124	0.17	0.179	0.168	0.102
F	0.012	0.255	0.179	0.292	0.208	0.150	0.169	0.166	0.1606	0.142	0.148	0.163
G	0.024	0.038	0.047	0.054	0.062	0.059	0.076	0.139	0.1452	0.152	0.175	0.195
H	0.017	0.031	0.046	0.051	0.048	0.059	0.071	0.082	0.1091	0.146	0.156	0.089

4.12 Crystal Violet assay for biofilm inhibition of *E. coli*



Fig 24: Crystal Violet assay to study biofilm inhibition of *E. coli*

Table 7: OD₅₇₀ of *E. coli* to determine Biofilm inhibition

	1	2	3	4	5	6	7	8	9	10	11	12
A	0.000	0.899	0.949	1.298	0.520	1.026	1.285	2.921	0.466	1.465	0.928	2.244
B	0.000	0.725	2.740	0.722	0.944	0.673	0.482	0.294	0.638	0.501	0.663	0.468
C	0.000	0.895	0.829	1.148	0.733	0.906	0.297	1.124	0.625	0.592	1.484	0.722
D	0.026	0.876	0.845	0.300	0.095	0.366	1.200	0.544	0.547	0.621	0.047	0.810
E	0.075	0.561	2.840	0.206	0.185	0.747	1.315	0.758	0.789	0.899	0.472	0.871
F	0.345	0.521	3.064	0.653	0.637	0.610	0.776	2.041	0.946	0.975	0.829	0.586
G	0.384	0.103	0.802	0.388	0.08	0.232	0.410	0.596	0.358	0.393	1.117	1.541
H	0.482	0.131	0.562	0.092	0.113	0.014	0.192	0.007	0.192	0.046	0.190	1.072

4.13 Crystal Violet assay for biofilm inhibition of *M. smegmatis*



Fig 25: Crystal Violet assay to study biofilm inhibition of *M. smegmatis*

Table 8: OD₅₇₀ of *M. smegmatis* to determine biofilm inhibition

	1	2	3	4	5	6	7	8	9	10	11	12
A	0.000	0.747	0.095	0.336	0.185	0.137	0.026	0.147	0.254	0.607	1.912	3.086
B	0.000	0.285	1.019	1.249	0.380	0.195	0.701	0.210	0.299	0.712	2.349	0.013
C	0.0000	0.937	0.104	0.717	1.609	0.563	2.457	0.998	1.362	0.449	0.666	0.075
D	0.159	2.661	1.257	0.632	0.746	0.016	0.919	1.312	0.417	0.596	0.140	0.468
E	0.434	0.417	0.775	1.971	1.208	0.636	0.442	2.504	2.002	0.345	1.517	0.844
F	0.023	2.934	1.096	0.383	0.705	3.179	1.426	1.500	0.651	2.012	0.881	0.748
G	0.235	1.046	1.100	0.521	0.980	1.099	0.883	0.104	0.076	0.526	0.435	0.269
H	1.170	0.944	0.383	0.622	0.459	1.848	0.585	0.434	0.273	0.323	0.317	0.2625

4.14 CFU count assay of Biofilm

Control and test well showed nearly same CFU when dilution and plating was performed; therefore no inhibition was shown by nanoparticles.

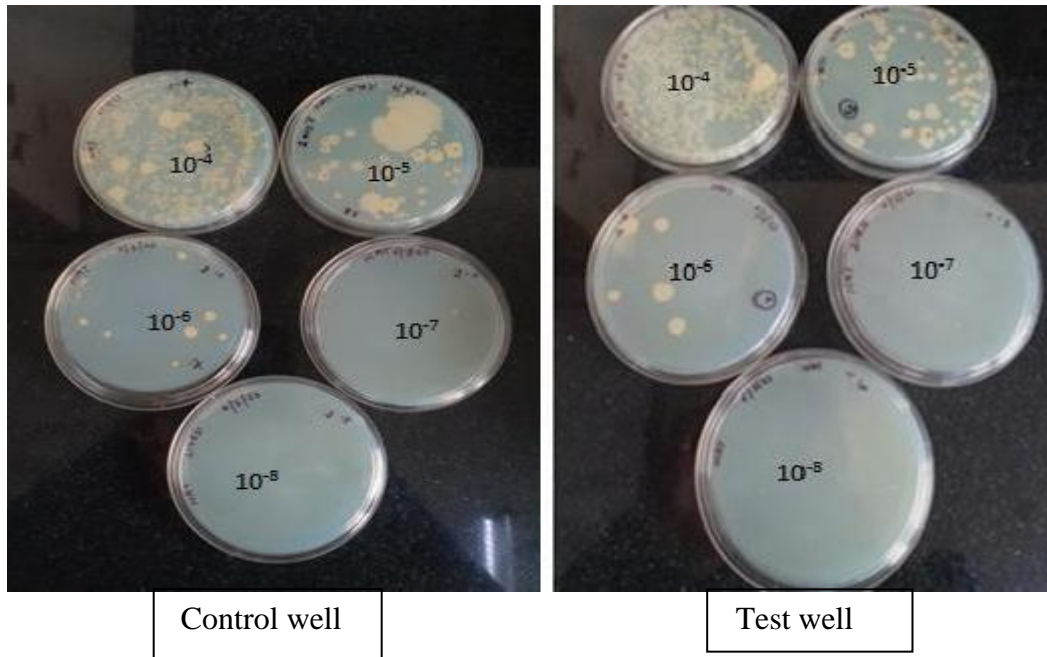


Fig 26: CFU Count assay of *M. smegmatis* biofilms

Table 9: CFU/ml in 10 fold dilutions of control and test wells for testing biofilm inhibition of *M. smegmatis*

Dilution Factor	Number of colonies in Control well	Number of colonies in test well
10^{-1}	Not countable	Not countable
10^{-2}	Not countable	Not countable
10^{-3}	Not countable	Not countable
10^{-4}	Not countable	Not countable
10^{-5}	347	355
10^{-6}	8	5
10^{-7}	No growth	No growth
10^{-8}	No growth	No growth

$$\begin{aligned} \text{CFU/mL}_{\text{Control}} &= \frac{347 \times 10^5}{0.1\text{mL}} \\ &= 3.47 \times 10^8 \end{aligned}$$

$$\begin{aligned} \text{CFU/mL}_{\text{Test}} &= \frac{355 \times 10^5}{0.1\text{mL}} \\ &= 3.55 \times 10^8 \end{aligned}$$

CHAPTER 4
DISCUSSION

Discussion:

Biological synthesis of nanoparticles from plant based material has gained so much of interest recently. These nanoparticles can offer antipyretic, antibacterial, antifungal as well as antioxidant activities. Especially plant having medical values is considered for synthesising nanoparticles, so that those phytochemical found in that plant adds on to the activity of nanoparticles [86]. This study focused on synthesis of AuNPs from water extraction of leaves of *W. somnifera*. Green AuNPs were synthesised by reducing metal salt of gold (Gold III Chloride) by plant extract. Nanoparticles were exposed to phytochemicals present in plant extract. Nanoparticles were exposed to phytochemicals present in plant extract during their nucleation phase and thus those ligands should have attached to nanoparticles surface.

Change in colour of reaction mixture gives an indication for formation of nanoparticles. Gold nanoparticles exhibited Surface Plasmon Resonance which give them ruby red to purple hue. The presence of nanoparticles was further confirmed by UV-VIS spectroscopy, which had shown a maximum peak between 540- 550. Alhumaydhi, have also reported similar kind of peak of gold nanoparticles synthesised using *Pistacia chinensis* [87].

The reduction of Au^{3+} ions took atleast 4 hours after addition of plant extract to 1M HAuCl_4 solution in a ratio of 7:1; which is indicated by change in colour of the reaction mixture.

FTIR spectroscopy was done to check the potential photochemical present in aqueous extract of *W. somnifera* leaves. Absorbance peak of both powdered and liquid sample were measured from 450 to 350 cm^{-1} . The data provided by FTIR showed the presence of C-H bond (alkanes), N-H (primary amines), and C-O (alcohols, carboxylic acid, esters or ethers) bond in correspondence to peak at 2093, 1630, and 1020 cm^{-1} respectively in powdered (solid) sample while single peak at 1637 cm^{-1} in liquid sample indicates the presence of primary amines in it. One more peak in liquid sample was seen at 3340 cm^{-1} which is due to presence of water molecules.

XRD graph of sample confirms the presence of crystalline gold nanoparticles in it. Peak values at 38.1, 44.3, 64.5 and 77.5. These peaks correspond to face centred cubic character of nanoparticles [86]. As per the data provided by zeta sizer, surface charge of nanoparticles was found to be -23mV which indicates slightly less stability of nanoparticles. According to a study by Bhattacharjee, 2016 nanoparticles with zeta potential greater than +25mV or less than -25mV tend to be stable and most appropriate for biomedical applications [88].

DLS data came out to be indicating hydrodynamic size of nanoparticles as 151.85 nm. Usually gold nanoparticles less than 100 nm are required for biomedical applications. Hydrodynamic size represent total size i.e. inorganic core coated with stern layer. For determination of actual size TEM analysis is required.

Antimicrobial activity of synthesised gold nanoparticles was examined using well diffusion (cup plate) method. They displayed a zone of 8.5 mm against *E. coli* (DH α) while when tested against *M. smegmatis* no potent inhibition was observed. It might be due to presence of mycolic acid in the cell wall of *M. smegmatis*. Shivraj et al ., 2020 reported antimycobacterial activity with a diameter of 13mm for zone of inhibition at 37 μ g/mL concentration of green synthesised silver chloride nanoparticles by commercial yeast extract [89].

Minimum Inhibitory Concentration (MIC) of nanoparticles and Plant extract of *W. somnifera* was tested using broth micro dilution method on 96- well microtiter plate, which does not showed killing of *E. coli* as well as for *M. smegmatis*. Maximum concentration of plant extract was 10mg/ml and that of AuNPs was 127 μ g/ml.

Biofilm inhibition assays were also performed by using same contents of microtiter plate which were used for testing MIC, those results also does not showed significant reduction in biofilm formation when compared with control wells.

Conclusion and Future prospects

In the current study we found that the 10mg/ml concentrated water extract of *W. somnifera* is unable to inhibit the growth of planktonic forms of *E.coli* as well as *M. smegmatis*. Gold nanoparticles synthesised by green synthesis method using *W. somnifera* extract showed antimicrobial activity against *E. coli* (DH5 α) while no such activity was observed against *M. smegmatis*. According to the objective of study efficacy of synthesised gold nanoparticles against biofilm formation was also tested but no significant inhibition in biofilm formation was observed for *E. coli* and *M. smegmatis*. It might be due to larger size of synthesised nanoparticles or may be due to lesser concentration of nanoparticles. We will be further working on decreasing the size by changing various parameters like temperature and pH.

CHAPTER 5
REFERENCES

References

1. I. Olsen, "Biofilm-specific antibiotic tolerance and resistance," *European Journal of Clinical Microbiology & Infectious Diseases*, vol. 34, no. 5, pp. 877–886, 2015.
2. W. M. Dunne, E. O. Mason, and S. L. Kplan, "Diffusion of rifampin and vancomycin through a *Staphylococcus epidermidis* biofilm," *Antimicrob. Agents Chemother*, vol. 37, pp. 2522–2526, 1993.
3. C. D. Nadell, K. Drescher, N. S. Wingreen, and B. L. Bassler, "Extracellular matrix structure governs invasion resistance in bacterial biofilms," *ISME J*, vol. 9, pp. 1700–1709, 2015.
4. B. Giwercman, E. T. Jensen, N. Høiby, A. Kharazmi, and J. W. Costerton, "Induction of β -lactamase production in *Pseudomonas aeruginosa* biofilm," *Antimicrob. Agents Chemother*, vol. 35, pp. 1008–1010, 1991.
5. P. S. Stewart, "Theoretical aspects of antibiotic diffusion into microbial biofilms," *Antimicrob. Agents Chemother*, vol. 40, pp. 2517–2522, 1996.
6. L. K. Jennings *et al.*, "Pel is a cationic exopolysaccharide that cross-links extracellular DNA in the *Pseudomonas aeruginosa* biofilm matrix," in *Proc. Natl. Acad. Sci*, vol. 112, USA, 2015, pp. 11353–11358.
7. K. M. Colvin *et al.*, "The Pel polysaccharide can serve a structural and protective role in the biofilm matrix of *Pseudomonas aeruginosa*," *PLoS Pathog*, 2011.
8. S. J. Amina and B. Guo, "A Review on the Synthesis and Functionalization of Gold Nanoparticles as a Drug Delivery Vehicle," *Int. J. Nanomed*, vol. 2020, pp. 9823–9857.
9. N. P. Nirmal, R. Mereddy, L. Li, and Y. Sultanbawa, "Formulation, characterisation and antibacterial activity of lemon myrtle and anise myrtle essential oil in water nanoemulsion," *Food Chem*, vol. 254, pp. 1–7, 2018.
10. T. T. Aung *et al.*, "Biofilms of pathogenic nontuberculous mycobacteria targeted by new therapeutic approaches," *Antimicrobial agents and chemotherapy*, vol. 60, no. 1, pp. 24–35, 2016.
11. L. Sshobley, C. Harkins, C. E. Macphee, and N. R. Stanley-Wall, "Giving structure to the biofilm matrix: an overview of individual strategies and emerging common themes," *FEMS Microbiol. Rev*, vol. 39, pp. 649–669, 2015.
12. H. C. Flemming and J. Wingender, "The biofilm matrix," *Nat. Rev. Microbiol*, vol. 8,

- pp. 623–633, 2010.
13. D. Santos Ramos *et al.*, “Nanotechnology-based drug delivery systems for control of microbial biofilms: a review,” *International journal of nanomedicine*, pp. 1179–1213, 2018.
 14. J. O. Adeyemi, A. O. Oriola, D. C. Onwudiwe, and A. O. Oyedeji, “Plant extracts mediated metal-based nanoparticles: Synthesis and biological applications,” *Biomolecules*, vol. 12, no. 5, p. 627, 2022.
 15. K. K. Jain, “Role of nanobiotechnology in drug delivery,” *Methods Mol. Biol.*, vol. 2059, pp. 55–73, 2020.
 16. M. Ramasamy and J. Lee, “Recent nanotechnology approaches for prevention and treatment of biofilm-associated infections on medical devices,” *Biomed Res. Int.*, vol. 2016, p. 1851242, 2016.
 17. A. Gupta, S. Pandey, and J. S. Yadav, “A review on recent trends in green synthesis of Gold nanoparticles for tuberculosis,” *Adv. Pharm. Bull.*, vol. 11, no. 1, pp. 10–27, 2021.
 18. K. Parveen, V. Banse, and L. Ledwani, “Green synthesis of nanoparticles: Their advantages and disadvantages,” in *AIP Conference Proceedings*, 2016.
 19. D. Sharma, L. Misba, and A. U. Khan, “Antibiotics versus biofilm: an emerging battleground in microbial communities,” *Antimicrob. Resist. Infect. Control*, vol. 8, no. 1, 2019.
 20. C. D. Nadell, K. Drescher, N. S. Wingreen, and B. L. Bassler, “Extracellular matrix structure governs invasion resistance in bacterial biofilms,” *The ISME journal*, vol. 9, no. 8, pp. 1700–1709, 2015.
 21. B. Giwercman, E. T. Jensen, N. Høiby, A. Kharazmi, and J. W. Costerton, “Induction of beta-lactamase production in *Pseudomonas aeruginosa* biofilm,” *Antimicrobial agents and chemotherapy*, vol. 35, no. 5, pp. 1008–1010, 1991.
 22. P. S. Stewart, “Theoretical aspects of antibiotic diffusion into microbial biofilms,” *Antimicrobial agents and chemotherapy*, vol. 40, no. 11, pp. 2517–2522, 1996.
 23. L. K. Jennings *et al.*, “Pel is a cationic exopolysaccharide that cross-links extracellular DNA in the *Pseudomonas aeruginosa* biofilm matrix,” *Proceedings of the National Academy of Sciences*, vol. 112, no. 36, pp. 11353–11358, 2015.
 24. M. Morikawa, “Beneficial biofilm formation by industrial bacteria *Bacillus subtilis*

- and related species,” *J. Biosci. Bioeng.*, vol. 101, no. 1, pp. 1–8, 2006.
25. M. E. Davey and A. George, “Microbial biofilms: From ecology to molecular genetics,” *Microbiol Mol Biol Rev*, vol. 64, no. 4, pp. 847–867, 2000.
 26. S. Sehar and I. Naz, “Role of the biofilms in wastewater treatment,” in *Microbial Biofilms - Importance and Applications*, InTech, 2016.
 27. K. Bosecker, “Bioleaching: metal solubilization by microorganisms,” *FEMS Microbiol. Rev.*, vol. 20, no. 3–4, pp. 591–604, 1997.
 28. R. D. I. Scott, “The Direct Medical Costs of Healthcare-Associated Infections,” *U. S*, 2009
 29. *29 Hospitals and the Benefits of Prevention. Division of Healthcare Quality Promotion*
 30. *30 National Center for Preparedness, Detection and Control of Infectious Diseases.*
 31. G. C. Ulett, J. Valle, C. Beloin, O. Sherlock, J. M. Ghigo, and M. A. Schembri, “Functional analysis of antigen 43 in uropathogenic *Escherichia coli* reveals a role in long-term persistence in the urinary tract,” *Infection and immunity*, vol. 75, no. 7, pp. 3233–3244, 2007.
 32. Q. Luo, J. Shang, X. Feng, X. Guo, L. Zhang, and Q. Zhou, “PrfA led to reduced biofilm formation and contributed to altered gene expression patterns in biofilm-forming *Listeria monocytogenes*,” *Current microbiology*, vol. 67, no. 3, pp. 372–378, 2013.
 33. J. A. Mohamed, F. Teng, S. R. Nallapareddy, and B. E. Murray, “Pleiotrophic Effects of 2 *Enterococcus faecalis* sagA-Like Genes, salA and salB Which Encode Proteins That Are Antigenic during Human Infection, on Biofilm Formation and Binding to Collagen Type I and Fibronectin,” *Journal of Infectious Diseases*, vol. 193, no. 2, pp. 231–240, 2006.
 34. J. A. Newman, C. Rodrigues, and R. J. Lewis, “Molecular Basis of the Activity of SinR Protein, the Master Regulator of Biofilm Formation in *Bacillus subtilis**♦,” *Journal of Biological Chemistry*, vol. 288, no. 15, pp. 10766–10778, 2013.
 35. A. Deep, U. Chaudhary, and V. Gupta, “Quorum sensing and bacterial pathogenicity: from molecules to disease,” *Journal of laboratory physicians*, vol. 3, no. 01, pp. 4–011, 2011.
 36. M. E. Davey, N. C. Caiazza, and G. A. Toole, “Rhamnolipid surfactant production

- affects biofilm architecture in *Pseudomonas aeruginosa* PAO1,” *Journal of bacteriology*, vol. 185, no. 3, pp. 1027–1036, 2003.
37. A. Kaur, N. Capalash, and P. Sharma, “Communication mechanisms in extremophiles: Exploring their existence and industrial applications,” *Microbiological research*, vol. 221, pp. 15–27, 2019.
38. N. Bagge *et al.*, “*Pseudomonas aeruginosa* biofilms exposed to imipenem exhibit changes in global gene expression and β -lactamase and alginate production,” *Antimicrob. Agents Chemother.*, vol. 48, no. 4, pp. 1175–1187, 2004
39. A. Moya-Beltran, C. Rojas-Villalobos, M. Diaz, N. Guiliani, R. Quatrini, and M. Castro, “Nucleotide second messenger-based signaling in extreme acidophiles of the *Acidithiobacillus* species complex: Partition between the core and variable gene complements,” *Front. Microbiol.*, vol. 10, 2019.
40. K. A. Coggan and M. C. Wolfgang, “Global regulatory pathways and cross-talk control *Pseudomonas aeruginosa* environmental lifestyle and virulence phenotype,” *Curr. Issues Mol. Biol.*, vol. 14, pp. 47–70, 2012
41. R. Hengge, “Principles of c-di-GMP signalling in bacteria,” *Nature Reviews Microbiology*, vol. 7, no. 4, pp. 263–273, 2009.
42. Y. Irie *et al.*, “Self-produced exopolysaccharide is a signal that stimulates biofilm formation in *Pseudomonas aeruginosa*,” *Proceedings of the National Academy of Sciences*, vol. 109, no. 50, pp. 20632–20636, 2012.
43. R. Jain, A. J. Behrens, V. Kaefer, and B. I. Kazmierczak, “Type IV pilus assembly in *Pseudomonas aeruginosa* over a broad range of cyclic di-GMP concentrations,” *J. Bacteriol.*, vol. 194, pp. 4285–4294, 2012.
44. R. Rajan and A. Shankar, “Features of the biochemistry of *Mycobacterium smegmatis*, as a possible model for *Mycobacterium tuberculosis*,” *Journal of Infection and Public Health*, vol. 13, no. 9, pp. 1255–1264, 2020.
45. “Role of hydrophobicity in bacterial adherence to carbon nanostructures and biofilm formation: Biofouling: Vol 26, No 3.” <https://www.tandfonline.com/doi/abs/10.1080/08927010903531491> (accessed May 07, 2023).
46. J. Esteban and M. García-Coca, “*Mycobacterium* Biofilms,” *Front. Microbiol.*, vol. 8, 2018, Accessed: May 07, 2023. [Online]. Available: <https://www.frontiersin.org/articles/10.3389/fmicb.2017.02651>

47. X. Xiang, W. Deng, M. Liu, and J. Xie, "Mycobacterium biofilms: factors involved in development, dispersal, and therapeutic strategies against biofilm-relevant pathogens," *Crit. Rev. Eukaryot. Gene Expr.*, vol. 24, no. 3, pp. 269–279, 2014.
48. D. S. Dhanjal *et al.*, "Mycology-Nanotechnology Interface: Applications in Medicine and Cosmetology," *Int. J. Nanomedicine*, vol. 17, pp. 2505–2533, Dec. 2022, doi: 10.2147/IJN.S363282.
49. A. I. Usman, A. Abdul Aziz, and O. Abu Noqta, "Application of green synthesis of gold nanoparticles: A review," *J. Teknol.*, vol. 81, no. 1, 2018.
50. B. A. Miu and A. Dinischiotu, "New green approaches in nanoparticles synthesis: An overview," *Molecules*, vol. 27, no. 19, p. 6472, 2022.
51. J. K. Patra *et al.*, "Nano based drug delivery systems: recent developments and future prospects," *J. Nanobiotechnology*, vol. 16, no. 1, p. 71, 2018.
52. S. Contera, J. Bernardino de la Serna, and T. D. Tetley, "Biotechnology, nanotechnology and medicine," *Emerg. Top. Life Sci.*, vol. 4, no. 6, pp. 551–554, 2020.
53. N. Baig, I. Kammakakam, and W. Falath, "Nanomaterials: a review of synthesis methods, properties, recent progress, and challenges," *Mater. Adv.*, vol. 2, no. 6, pp. 1821–1871, 2021.
54. G. A. Silva, "Introduction to nanotechnology and its applications to medicine," *Surg. Neurol.*, vol. 61, no. 3, pp. 216–220, 2004.
55. V. Harish *et al.*, "Nanoparticle and nanostructure synthesis and controlled growth methods," *Nanomaterials (Basel)*, vol. 12, no. 18, p. 3226, 2022.
56. I. Ielo *et al.*, "Synthesis, chemical-physical characterization, and biomedical applications of functional gold nanoparticles: A review," *Molecules*, vol. 26, no. 19, p. 5823, 2021.
57. C. Gutiérrez-Wing, J. J. Velázquez-Salazar, and M. José-Yacamán, "Procedures for the synthesis and capping of metal nanoparticles," *Methods Mol. Biol.*, vol. 906, pp. 3–19, 2012.
58. A. Rana, K. Yadav, and S. Jagadevan, "A comprehensive review on green synthesis of nature-inspired metal nanoparticles: Mechanism, application and toxicity," *J. Clean. Prod.*, vol. 272, no. 122880, p. 122880, 2020.
59. Z. Jiang, L. Li, H. Huang, W. He, and W. Ming, "Progress in laser ablation and biological synthesis processes: 'top-down' and 'bottom-up' approaches for the Green

- synthesis of Au/Ag nanoparticles,” *Int. J. Mol. Sci.*, vol. 23, no. 23, p. 14658, 2022.
60. F. Khan, M. Shariq, M. Asif, M. A. Siddiqui, P. Malan, and F. Ahmad, “Green nanotechnology: Plant-mediated nanoparticle synthesis and application,” *Nanomaterials (Basel)*, vol. 12, no. 4, p. 673, 2022.
61. K. K. Bharadwaj *et al.*, “Green synthesis of gold nanoparticles using plant extracts as beneficial prospect for cancer theranostics,” *Molecules*, vol. 26, no. 21, p. 6389, 2021.
62. “Gold nanoparticles: preparation, properties, and applications in bionanotechnology - Nanoscale (RSC Publishing).” <https://pubs.rsc.org/en/content/articlelanding/2012/nr/c1nr11188d/unauth> (accessed May 08, 2023).
63. A. Saqr *et al.*, “Synthesis of gold nanoparticles by using green machinery: Characterization and in vitro toxicity,” *Nanomaterials*, vol. 11, no. 3, 2021.
64. C. Tao, “Antimicrobial activity and toxicity of gold nanoparticles: research progress, challenges and prospects,” *Lett. Appl. Microbiol.*, vol. 67, no. 6, pp. 537–543, 2018.
65. D. B. Shinde, R. Pawar, J. Vitore, D. Kulkarni, S. Musale, and P. Giram, “Natural and synthetic functional materials for broad spectrum applications in antimicrobials, antivirals and cosmetics,” *Polym. Adv. Technol.*, vol. 32, no. 11, pp. 4204–4222, 2021.
66. X. Zhan, J. Yan, H. Tang, D. Xia, and H. Lin, “Antibacterial properties of gold nanoparticles in the modification of medical implants: A systematic review,” *Pharmaceutics*, vol. 14, no. 12, p. 2654, 2022.
67. “kong
68. S. Tarantino, A. P. Caricato, R. Rinaldi, C. Capomolla, and V. De Matteis, “Cancer treatment using different shapes of gold-based nanomaterials in combination with conventional physical techniques,” *Pharmaceutics*, vol. 15, no. 2, 2023.
69. C. Pimentel *et al.*, “Human pleural fluid and human serum albumin modulate the behavior of a hypervirulent and multidrug-resistant (MDR) *Acinetobacter baumannii* representative strain,” *Pathogens*, vol. 10, no. 4, p. 471, 2021.
70. I. E. Mba and E. I. Nweze, “Nanoparticles as therapeutic options for treating multidrug-resistant bacteria: research progress, challenges, and prospects,” *World J. Microbiol. Biotechnol.*, vol. 37, no. 6, p. 108, 2021.
71. A. S. Joshi, P. Singh, and I. Mijakovic, “Interactions of gold and silver nanoparticles with bacterial biofilms: Molecular interactions behind inhibition and resistance,” *Int.*

- J. Mol. Sci.*, vol. 21, no. 20, 2020.
72. S. Paul *et al.*, “Withania somnifera (L.) Dunal (Ashwagandha): A comprehensive review on ethnopharmacology, pharmacotherapeutics, biomedical and toxicological aspects,” *Biomed. Pharmacother.*, vol. 143, no. 112175, p. 112175, 2021.
73. R. Dutta, R. Khalil, R. Green, S. S. Mohapatra, and S. Mohapatra, “Withania Somnifera (ashwagandha) and Withaferin A: Potential in integrative oncology,” *Int. J. Mol. Sci.*, vol. 20, no. 21, p. 5310, 2019.
74. Y. R. Perera, R. A. Hill, and N. C. Fitzkee, “Protein interactions with nanoparticle surfaces: Highlighting solution NMR techniques,” *Isr. J. Chem.*, vol. 59, no. 11–12, pp. 962–979, 2019.
75. M. A. El-Sayed, “Small is different: Shape-, size-, and composition-dependent properties of some colloidal semiconductor nanocrystals,” *Acc. Chem. Res.*, vol. 37, no. 5, pp. 326–333, 2004.
76. Y. R. Perera, R. A. Hill, and N. C. Fitzkee, “Protein interactions with nanoparticle surfaces: Highlighting solution NMR techniques,” *Isr. J. Chem.*, vol. 59, no. 11–12, pp. 962–979, 2019.
77. Y. Fan, M. Marioli, and K. Zhang, “Analytical characterization of liposomes and other lipid nanoparticles for drug delivery,” *J. Pharm. Biomed. Anal.*, vol. 192, no. 113642, p. 113642, 2021.
78. S. Mourdikoudis, R. M. Pallares, and N. T. K. Thanh, “Characterization techniques for nanoparticles: comparison and complementarity upon studying nanoparticle properties,” *Nanoscale*, vol. 10, no. 27, pp. 12871–12934, 2018.
79. N. K. Thakral, R. L. Zanon, R. C. Kelly, and S. Thakral, “Applications of powder X-ray diffraction in small molecule pharmaceuticals: Achievements and aspirations,” *J. Pharm. Sci.*, vol. 107, no. 12, pp. 2969–2982, 2018.
80. Y. A. Hussein and J. M. Mansour, “Synthesis of gold and copper nanomaterials by pulsed laser ablation method,” *Diyala J. Pure Sci.*, vol. 18, no. 4, pp. 57–70, 2022.
81. S. Rades *et al.*, “High-resolution imaging with SEM/T-SEM, EDX and Sam as a combined methodical approach for morphological and elemental analyses of single engineered nanoparticles,” *RSC Adv.*, vol. 4, no. 91, pp. 49577–49587, 2014. doi:10.1039/c4ra05092d
82. M. Malatesta, “Transmission electron microscopy as a powerful tool to investigate the interaction of nanoparticles with subcellular structures,” *International Journal of*

- Molecular Sciences*, vol. 22, no. 23, p. 12789, 2021. doi:10.3390/ijms222312789
83. I. H. Lone, J. Aslam, and A. Akhter, "Characterization of advanced green materials," *Advanced Green Materials*, pp. 31–41, 2021. doi:10.1016/b978-0-12-819988-6.00003-3
84. Y. Rao, G. K. Inwati, and M. Singh, "Green synthesis of capped gold nanoparticles and their effect on Gram-positive and Gram-negative bacteria," *Future Sci. OA*, vol. 3, no. 4, p. FSO239, 2017.
85. A. Sharma, J. Vashist, and R. Shrivastava, "Response surface modeling integrated microtiter plate assay for *Mycobacterium fortuitum* biofilm quantification," *Biofouling*, vol. 37, no. 8, pp. 830–843, 2021.
86. J. Shanmugapriya *et al.*, "Green synthesis of copper nanoparticles using *Withania somnifera* and its antioxidant and antibacterial activity," *J. Nanomater.*, vol. 2022, pp. 1–9, 2022.
87. F. A. Alhumaydhi, "Green Synthesis of Gold Nanoparticles Using Extract of *Pistacia chinensis* and Their In Vitro and In Vivo Biological Activities," *J. Nanomater.*, vol. 2022, p. 5544475, Jun. 2022, doi: 10.1155/2022/5544475.
88. S. Bhattacharjee, "DLS and zeta potential-what they are and what they are not?," *J. Controlled Release*, vol. 235, pp. 337–351, 2016.
89. A. Sivaraj, V. Kumar, R. Sunder, K. Parthasarathy, and G. Kasivelu, "Commercial yeast extracts mediated green synthesis of silver chloride nanoparticles and their anti-mycobacterial activity," *J. Cluster Sci.*, vol. 31, no. 1, pp. 287–291, 2020.

CHAPTER 6

APPENDIX

APPENDIX

6.1 Growth media for bacterial culture

Media was prepared in Milli-Q water and autoclaved at 15 psi (1.05 kg/cm²) for 20 min [on liquid cycle].

6.1.1 LB medium (Luria-bertani medium) [pH = 7.4]

Tryptone	10 g
Yeast extract	5 g
NaCl	10 g

Components were dissolved in 1000 mL Milli-Q water. Solid media was prepared by adding 1.5 % agar

6.1.2 LBGT (LB broth with glycerol and Tween 80) [pH = 7.4]

LB broth	1000 mL
Glycerol	0.5 % (v/v)
Tween 80	0.15 % (v/v)

6.1.3 Nutrient medium (broth) [pH = 7.4]

Peptone	5 g
Yeast extract	1.5 g
Beef extract	1.5 g
NaCl	5 g

Components were dissolved in 1000 mL Milli-Q water. Solid media was prepared by adding 1.5 % agar.

6.1.4 Nutrient agar Tween 80 (NAT) [Agar = 1.5 % (w/v)]

Nutrient broth	13 g / 1000 mL Milli-Q water
Tween 80	0.05 % (v/v)

6.2 Reagents for Ziehl-Neelsen (acid-fast) staining

6.2.1 Basic fuchsin (primary stain)

Basic fuchsin	3g
Phenol	5 % (v/v)
Ethanol (96%)	10 mL

5 % phenol was added to 3g basic fuchsin (dissolved in 10 mL of 96 % ethanol). The volume was adjusted to 100 mL using Milli-Q water. The solution was filtered through Whatman filter paper No. 1.

3.2.2 Acid alcohol (decolourizer)

3.2.3 3 mL HCl (concentrated) was added to 97 mL 96% ethanol.

6.2.3 Malachite green (counter stain)

Malachite green	0.25 g
Milli-Q water	100 mL (final volume)

The mixture was stirred to dissolve the solute, and filtered through Whatman filter paper No. 1.

6.3 Normal saline [8.5 g NaCl was dissolved in 1000 mL Milli-Q water]

6.4 Tween normal saline (TNS) [Final volume make-up = 1000 mL, using Milli-Q water]

NaCl	9 g
Tween 80	0.1 % (v/v)

6.5 1M HAuCl₄

Gold(III) Chloride	15.16mg
Millipore Water	100ml

6.6 0.5Mc Farland solution

1% BaCl ₂	0.05ml
1.175% H ₂ SO ₄	9.95ml

CHAPTER 7
PUBLICATIONS

1. INHIBITION OF BIOFILM-FORMING DRUG-RESISTANT PATHOGENIC BACTERIA USING GOLD NANOPARTICLES

Nidhi Tyagi, Ayushi Sharma, Rahul Shrivastava

Poster Presentation at VI International Conference on Advances in Biosciences. & Biotechnology (ICABB-2023) organised by JIIT, Noida from January 18-20, 2023

2. INHIBITION OF BIOFILM-FORMING DRUG-RESISTANT PATHOGENIC BACTERIA USING GOLD NANOPARTICLES

Nidhi Tyagi, Rahul Shrivastava

Poster Presentation in 2nd National Science Day Symposium organised by Jaypee University of Information and Technology, Solan, HP on February 24, 2023

3. Optimization of protocol for quantification of biofilm formed by pathogenic rapidly- growing nontuberculous mycobacteria for diagnostic screening in

Ayushi Sharma, **Nidhi Tyagi**, Rahul Shrivastava

Book chapter submitted to Methods In Microbiology VOL. 53